UNIVERSITÀ DEGLI STUDI DI NAPOLI “FEDERICO II”

DIPARTIMENTO DI SCIENZE DELLA TERRA DELL’AMBIENTE E DELLE RISORSE

DOTTORATO IN
“GEOLOGIA STRUTTURALE”

XXXVI CICLO

# THE ANALYSIS OF FAULT ZONES IN VOLCANIC AND OROGENIC AREAS OF THE SOUTHERN APENNINES

COORDINATORE

Ch.ma Prof. ssa Rosa Di Maio

CANDIDATO

Dott. Renato Diamanti

TUTOR

Prof. Stefano Vitale

Co-TUTORS

Prof. Giacomo Russo
Dr. Giovanni Camanni

## FOREWORD

The PhD research is focused on the study of fault zones exposed in the Campi Flegrei caldera and carbonates in the southern Apennines. Initially, the project was planned to be a study on fault zones in orogenic settings. However, during the first PhD year, owing to the COVID-19 pandemic, fieldwork was restricted exclusively to the Campi Flegrei area due to travel restrictions imposed by emergency regulations. Therefore, we strategically decided to convert limitation into an opportunity by turning our research efforts to investigate gravitational faults in volcanic environments. Following the decadence of emergency regulations and the completion of one year within the PhD program, our research scope expanded to encompass the study of fault zones within the Triassic dolomites in the southern Apennines. These endeavors aimed to explore fault zones across various geodynamic settings, specifically within volcanic and orogenic settings, examining deformation structures at outcrops and microscales. Furthermore, in my final year of the Ph.D. program, I delved into the fascinating field of micromechanical characterization of dolomite textures. This period was dedicated to thoroughly exploring the interplay between dolomite textural, mechanical and structural relationships. In this research, we made efforts to depict the various constitutive attributes of fault zones, encompassing fault geometry, fault rock fabric, distribution of fault displacement, and processes implying fluid-rock interaction within exposed fault zones in the Campi Flegrei caldera and the southern Apennines. The principal outcomes of this research could be helpful in the understanding of how these faults influence fluid flow, whether enhancing or inhibiting it, within both volcanic and orogenic geological settings. Furthermore, by exploring the intricate interplay between rock texture and deformation mechanisms, we have illuminated the evolutionary dynamics of microfracture patterns within dolostones.

# Table of Contents


**INTRODUCTION** **6**

**CHAPTER I** **11**

**1. COLLAPSE FAULTS IN THE CAMPI FLEGREI VOLCANO** **11**

***1.1 Faults in volcanic areas*** *11*

***1.2 Campi Flegrei volcano*** *12*

***1.3 Virtual outcrop modelling*** *16*

***1.4 Fault zone structure and throw analysis*** *17*

**1.4.2 Throw analysis** 19

***1.5. Kinematic coherence of the fault array*** *20*

**CHAPTER II** **26**

**2. POLY-DEFORMED FAULT ZONE DEVELOPED WHITIN NORIAN DOLOMITES IN THE SOUTHERN APENNINES** **26**

***2.1 Poly-deformed fault zone*** *26*

***2.2 Tectonic evolution of the southern Apennines*** *28*

***2.3 Stratigraphic and structural setting of the Matese Massif*** *28*

**3. SUCCESSIVE FAULTING EVENTS AND FAULT KINEMATICS** **31**

***3.1 Ailano fault zone*** *32*

**6. INTERPLAY OF DOLOMITE TEXTURES AND FAULTING: INSIGHTS FROM MESOZOIC WESTERN ADRIA TECTONIC EVOLUTION** **34**

**CHAPTER III** **35**

**7. FRACTURE PATTERN IN DOLOMITES WITH VARYING GRAIN SIZE DISTRIBUTION** **35**

***7.1 Textural control on carbonate rock strength and fractures patterns*** *35*

***7.2 Sampling sites*** *36*

***7.3 Sampling and experimental procedures*** *38*

**7.3.1 Petrographic analysis** 38

**7.3.2 Mechanical and porosity analysis** 39

**7.3.3 Failure mode characterization** 40

**8. FINAL CONCLUSIONS** **41**

**REFERENCES** **43**

*Questa tesi è il risultato di tre anni di lavoro bellissimi che mi hanno insegnato l'impagabile bellezza della ricerca nelle Scienze della Terra. In questi anni sono state molte le persone che hanno arricchito la mia esperienza di importantissimi insegnamenti scientifici e, soprattutto, di vita.*

*Anche se ringraziarli tutti sarebbe uno sforzo perfino maggiore di quello che mi ha richiesto scrivere la tesi, vale assolutamente la pena fare un tentativo.*

*Il primo pensiero non può che essere rivolto ai miei mentori Prof. Stefano Vitale, Dr. Giovanni Camanni e il Prof. Giacomo Russo che con i loro preziosi insegnamenti, suggerimenti e soprattutto rimproveri, mi hanno trasmesso la dedizione e l'umiltà necessaria per diventare un buon ricercatore. A voi devo, più che i miei ringraziamenti, la possibilità di aver vissuto un'esperienza accademica estremamente positiva.*

*Vorrei anche esprimere la mia più sincera gratitudine nei confronti di tutto il personale tecnico-scientifico e i responsabili dei numerosi laboratori in cui ho avuto il previlegio di poter passare moltissime ore apprendendo il genio del saper fare.*

*Un pensiero e i miei complimenti vanno anche ai miei colleghi del XXXVI ciclo di dottorato Roberto, Rosanna, Daniele, Antonio e Muhammad. Perché con voi le chiacchierate davanti ai caffè erano più interessanti di molti convegni.*

*A Napoli che adottandomi come uno dei suoi tanti figli mi ha insegnato il valore della vera accoglienza. Napoli è un'emozione troppo grande per non essere condivisa!*

*Ai miei cari che non mi ha mai fatto mancare il loro sostegno ovunque loro fossero, ovunque io fossi!*

*A te che hai reso tutto questo possibile.*

## INTRODUCTION

In the shallow crust, faults and fractures are formed in a wide variety of geodynamic settings, including subduction zones, accretionary prisms, fold and thrust belts, passive margins (Turcotte, 2002 and references therein) and volcanic areas (Acocella, 2010 and references therein). Numerous geological studies focused on the description and interpretation of fault zone geometry, architecture and evolution to understand and predict the impact of faults on fluid flow in the upper crust, including groundwater flow (Bense et al., 2013; Gudmundsson, 2000), hydrocarbon migration, entrapment and production (Knipe et al., 1998; Grauls et al., 2002; Sorkhabi and Tsuji, 2005; Manzocchi et al., 2010; Wibberley et al., 2017), hydrothermal flow and mineralization (Rowland and Sibson, 2004; Person et al., 2008; Fairley, 2009), as well as dyke and sill emplacement (Waite and Smith, 2002; Mathieu et al., 2008; White et al., 2011; Trippanera et al., 2015, 2019). Furthermore, at shallow crustal depths, where low-temperature and low-pressure conditions are effective, the stress-deformation processes can trigger earthquake nucleation (Lockner and Beeler, 2002 and references therein) and transfer or eruption of shallow magma (Acocella, 2021 and reference therein) in all tectonic regimes. For these reasons, the characterization of fault zones developed in volcanic and orogenic regions through structural and microstructural analyses, provides important evidence for describing deformation processes and rocks' dynamic behaviors related to volcanic and tectonic processes.

In recent years, the study of fault zones has made significant progress and become the main object of a prolific scientific branch. This is because the study of faults in volcanic and mountain regions is important respectively for geothermal and hydrocarbon industries (Bodvarsson et al., 1982; Dholakia et al., 1998; Aydin, 2000; Agosta and Aydin, 2006; Agosta et al., 2007; Tondi, 2007; Manzocchi et al., 2010; Wibberley et al., 2017; Liang et al., 2018; Jolie et al., 2021) as well as for mitigating risk connected to seismic and volcanic hazards (Wesnousky, 1986; Ventura and Vilardo, 1999; Scholz and Gupta, 2000; Tuffen and Digwell, 2005; Orsi et al., 2004; McCaplin, 2009; Marti and Felpeto, 2010; Alberico et al., 2011; Wicks et al., 2011; Scholz, 2019). Moreover, recent studies on fault zone permeability (Antonellini and Aydin, 1994; Ghisetti and Vezzani, 2002; Agosta and Kirschner, 2003; Micarelli et al., 2006; Agosta et al., 2007; Bense et al., 2013; Walker et al., 2013; Scibek, 2020; Curzi et al., 2024; Rizzo et al., 2024), fluid-rock interaction processes (Evans and Chester, 1985; Sibson, 2000; Faulkner et al., 2010; Duan et al., 2016), grain shape and size evolution with slip (Storti et al., 2007; Ferraro et al., 2018) and throw distribution (Camanni et al., 2019, 2023; Delogkos et al., 2020; Roche et al., 2021) obtained from both laboratory simulated faults (Schopfer et al., 2006, 2016; Han et al., 2007; Abe et al., 2011) and meso- and microstructural studies (Smeraglia et al., 2017; Shuck et al., 2018, 2020) have improved our understanding of the mechanical and hydraulic behavior of fault zones.

This PhD thesis aims to delineate the complex relationships between deformation processes occurring within poly-deformed brittle deformation zones and their consequential impact on subsurface fluid flow, mainly focusing on volcanic and fold and thrust belt regions. Several differences, among others, characterize faults developed in volcanic and in fold and thrust belt areas: i) origin and mechanisms, iii) fault rock composition and iv) associated geological landforms. Faults origin within volcanic regions is primarily attributed to volcanic activity, including magma intrusion, volcanic inflation/deflation, dyke emplacement and gravitational collapses related to volcanic processes (Acocella, 2007; Trippanera et al., 2015; Gudmundsson, 2020). Conversely, faults developed in non-volcanic areas typically form due to plate tectonics in all tectonic settings, such as divergent boundaries (such as mid-ocean ridges), convergent boundaries (such as subduction zones and mountain ranges) and transform plate-boundaries (Tchalenko, 1970; Sibson, 1981). Moreover, faults in volcanic regions may exhibit complex kinematic, including synchronous normal and reverse faults resulting in intricate geometries such as ring faults around collapsed calderas (Acocella, 2007; Gudmundsson, 2020). On the contrary, tectonic faults often show more uniform kinematic (i.e., normal, reverse and transform) and may display simpler geometry based on the type of tectonic forces (Ramsay and Huber, 1987; Jackson and Mckenzie, 1983; Martel, 1999; Duan and Oglesby, 2005;

Childs et al., 2017).

The composition of fault rocks can be significantly different in fault zones within volcanic and non-volcanic regions. In volcanic regions, fault rocks exhibit homogeneous composition due to their association with volcanic materials, usually showing alteration by hot fluids and volcanic gasses (Tibaldi and Groppelli, 2002; Branney and Acocella, 2015). Fault rocks in non-volcanic regions are more heterogeneous because they display compositions influenced by the types of rocks they deform (i.e., shale, sandstone, dolostone, etc..) (Ramsay and Huber, 1987; Passchier and Trouw, 2005). Moreover, the differences in host-rock mechanical properties can profoundly influence nucleation and propagation mechanisms of the brittle deformation structures (e.g., faults and fractures) (Ferrill and Morris, 2008; Laubach et al., 2009).

Finally, appreciable differences between fault zones in orogenic and volcanic areas are represented by relative landscape geomorphologies. In volcanic regions, faults can be associated with specific volcanic landforms like diatremes, pit craters, volcanic cones and, most importantly, calderas (Corazzato and Tibaldi, 2006; Branney and Acocella, 2015; Ferrill et al., 2016; Gómez-Vasconcelos et al., 2020). While in other geological contexts, faults shape mountain ranges and valleys depending on the fault kinematics (Bishop, 2007; Kirby and Whipple, 2012; Whittaker, 2012). The PhD thesis is divided into three chapters, each one exploring different aspects of brittle deformation in volcanic and fold and thrust belt regions and their influence on brittle strain accommodation and fluid-rock interaction processes:

1. **Investigating gravitational faults related to magma migration within the Campi Flegrei volcano**

   The initial part of the thesis is dedicated to examining the interplay between gravitational fault development and the subsurface migration of magma likely preceding the latest volcanic eruption in the Campi Flegrei caldera (i.e., Monte nuovo eruption 1538 CE). This investigation aims to unravel the connections between fault evolution and the dynamics of magma transfer at depth.

2. **Study of fault zones within Triassic dolomite in the southern Apennines:**

The subsequent part focuses on analyzing fault zones within the Triassic dolomite prominently exposed in the southern Apennines. Specifically, our research focuses on poly-deformed fault zones situated on the southwestern flank of the Matese Massif. Within this region, two distinct outcrops have been selected to study fault zones in relation to:

I. ***Characterization of geometry and deformation mechanisms of superposed fault zones***

This section involves a detailed characterization of an inherited fault zone, aiming at describing the role of texture and strength of inherited fault rock units on the geometry and deformation mechanisms of the superposed faults. By understanding how the texture and strength of inherited fault rocks influence subsequent faulting processes, this research aims to provide predictive indicators regarding fluid flow behavior and fault integrity within complex fault systems. Such predictive capabilities hold crucial implications for various applications, including reservoir characterization and assessment of subsurface fluid migration in geological settings characterized by multiple deformations.

II. ***Investigation of fault-driven hydrothermal saddle dolomitization***

This section is dedicated to the detailed study of the hydrothermal mineralizing fluids active during deformation along Upper Triassic-Lower Jurassic normal faults. A primary innovation of this research lies in its description of fault-driven hydrothermal saddle dolomitization since it is the first time that hydrothermal fluid circulation along normal fault is linked to Pangea breakup in the southern Apennines.

Notably, identifying hydrothermal minerals indicative of high-temperature circulating fluids, coupled with isotopic ratio analysis (i.e., radiogenic and stable isotopes), offer evidence suggesting a plausible involvement of magmatic sources in the hydrothermal system. This evidence represents a significant novelty in the tectonic reconstruction of the southwestern Adria margin during the Late Triassic-Early Jurassic period. Moreover, this research not only sheds light on the occurrence of hydrothermal processes linked to fault deformation but also introduces evidence of the potential interplay between magmatic sources and hydrothermal systems in the Mesozoic geological evolution of the southern Apennines. Such novel insights have implications for geological tectonic studies and the broader understanding of geological processes associated with fault-related hydrothermal systems.

3. **Characterization of fracture pattern evolution in dolomites with varying grain size distribution**

   This segment is dedicated to comprehensively examining the uniaxial compressive strength, failure mode, and microfracture patterns exhibited by dolostones featuring diverse grain size distributions. The study conducted an in-depth analysis of the textural attributes of three distinct dolostone samples collected from various locations in the southern Apennines. The experimental procedures encompassed the detailed characterization of secondary porosity and fracture patterns in dolomite samples after failure induced by uniaxial compression. This study specifically investigates the relationships between micro-fracture patterns, secondary porosity, and variation in dolomite grain size. The findings of this study can hold significant application for predicting the strength of dolomitic rocks in geotechnical studies and for refining the quality assessment of reservoirs within deformed dolostone.

This comprehensive exploration aims to deepen our understanding of fault-related stress-deformation processes and their implication for fluid migration in geologically diverse settings, offering valuable insights into the complex relationships between deformation and fluid flow within the shallow Earth's crust.

# CHAPTER I

# 1. COLLAPSE FAULTS IN THE CAMPI FLEGREI VOLCANO

## 1.1 Faults in volcanic areas

Faults within volcanic regions exhibit diverse origins and forms to facilitate deformation resulting from a variety of volcano-tectonic processes (Gudmundsson, 2020). These faults can arise to accommodate various phenomena, such as uplift or subsidence linked to volcano-tectonic inflation and deflation episodes (Gudmundsson, 1988, 2008). Additionally, fault development may occur due to intrusions like dikes and sills (Trippanera et al., 2015; 2019) or pressure fluctuations within the shallow plumbing system (Intrieri et al., 2013; Tibaldi and Groppelli, 2002; Walter et al., 2005). Moreover, faults in volcanic areas can emerge along the flanks of volcanoes due to gravitational instability induced by the processes above (McGuire, 2003). A unique category of faults is those that develop to accommodate gravitational collapses triggered by various volcano-tectonic processes, such as magma migration or withdrawal from magma chambers (Acocella, 2007; Branney, 1995; Branney and Acocella, 2015; Walker, 1984; Burchardt and Walter, 2010; Kennedy et al., 2004). Specifically, faults that facilitate gravitational collapses often exhibit steep inclinations and can demonstrate simultaneous movements characterized by normal and reverse senses (Cole et al., 2005; Geyer and Martì, 2014; Roche et al., 2000; Tepp, 2021). For instance, faults accommodating caldera collapses frequently adopt an arcuate and concentric configuration (ring faults) encircling the collapsed area (Cole et al., 2005; Geyer and Martì, 2014; Roche et al., 2000; Tepp, 2021). Additionally, faults in volcanic regions can also form to facilitate the development of diatremes (Isaia et al., 2015; Lorenz, 1975, 1986; Lorenz and Kurszlaukis, 2007) and pit craters (Holohan et al., 2011). Therefore, it is not always straightforward to determine the origin of faults found in a volcanic area. Nevertheless, determining their origin can be critical, for example, for seismic hazard assessment and estimating their geothermal potential. Furthermore, faults with different origins can influence the fluid uprise pathways, the anomalies in the heat flow, and the hydrothermal alteration of the rock rheologic properties (Siler et al., 2016; Heap et al., 2020; Isaia et al., 2021).

In this part, we thoroughly analyzed a fault array exposed in cross-section within the active Campi Flegrei caldera (CFc) of southern Italy. The exceptional outcrop conditions and the thinly-bedded nature of the faulted volcanic succession provided a unique opportunity to meticulously characterize the structural aspects and displacement distribution within the fault array. Through comprehensive geometric and displacement analyses of this array and considering the geological context of the CFc, we propose a model. According to this model, the formation of the studied fault array was likely driven by the need to accommodate a gravitational collapse triggered by subterranean lateral magma migration, predating the historical Monte Nuovo eruption in 1538 CE.

### 1.2 Campi Flegrei volcano

The study area is located within the central sector of the Campi Flegrei caldera, an active volcano emplaced along the Tyrrhenian side of the southern Apennines (southern Italy) (Vitale and Ciarcia, 2013 and references therein, **Fig. 1.1a**). The CFc is located in the westernmost sector of the southern Apennines, within the Plio-Pleistocene Campania Plain (Cinque et al., 1993), where starting from 250 ka, the crustal extension related to the back-arc opening of the Tyrrhenian Sea (Vitale and Ciarcia, 2013) induced intense volcanic activity. Since 200 ka ago, volcanic activity focused in the Campi Flegrei, Ischia and Procida volcanos that form the Phlegrean Volcanic District.

Recent observations in the CFc have identified extensive ESE-WNW trending faults that intersect both the youngest volcanic successions and pre-existing deformation structures (Vitale and Isaia, 2014; Natale et al., 2020; 2021; Vitale et al., 2019; Isaia et al., 2021). Specifically, the CFc represents a nested depression (**Fig. 1.1a**) formed subsequent to the Plinian eruptions of the Campanian Ignimbrite around 39.8 thousand years ago (Giaccio et al., 2008), followed by the younger Neapolitan Yellow Tuff eruption approximately 14.9 thousand years ago (Deino et al., 2004). Following these major eruptions, the CFc witnessed several eruptions of varying intensities (Isaia et al., 2004, 2015;

Vitale et al., 2019). These eruptions included the formation of the Agnano-Monte Spina nested caldera (AMS, 4.55 thousand years ago), the Solfatara maar-diatreme (SOL, 4.28 thousand years ago), and the Astroni crater (AST, 4.2 thousand years ago). The most recent historically documented eruption occurred in 1538 CE, resulting in the formation of the Monte Nuovo volcano (**Fig. 1.1a**). This eruption was preceded by several meters of ground deformations originating in Pozzuoli and subsequently shifting westward after a magma transfer (Di Vito et al., 2016). Notably, this eruption was accompanied by intense faulting and fracturing (Bevilacqua et al., 2020). Since 2005, the CFc has experienced ground uplift, with the current peak ground deformation reaching 90 cm, predominantly localized within the Rione Terra of Pozzuoli town. This uplift has coincided with an escalation in hydrothermal activity and seismic events (e.g., Isaia et al., 2021).

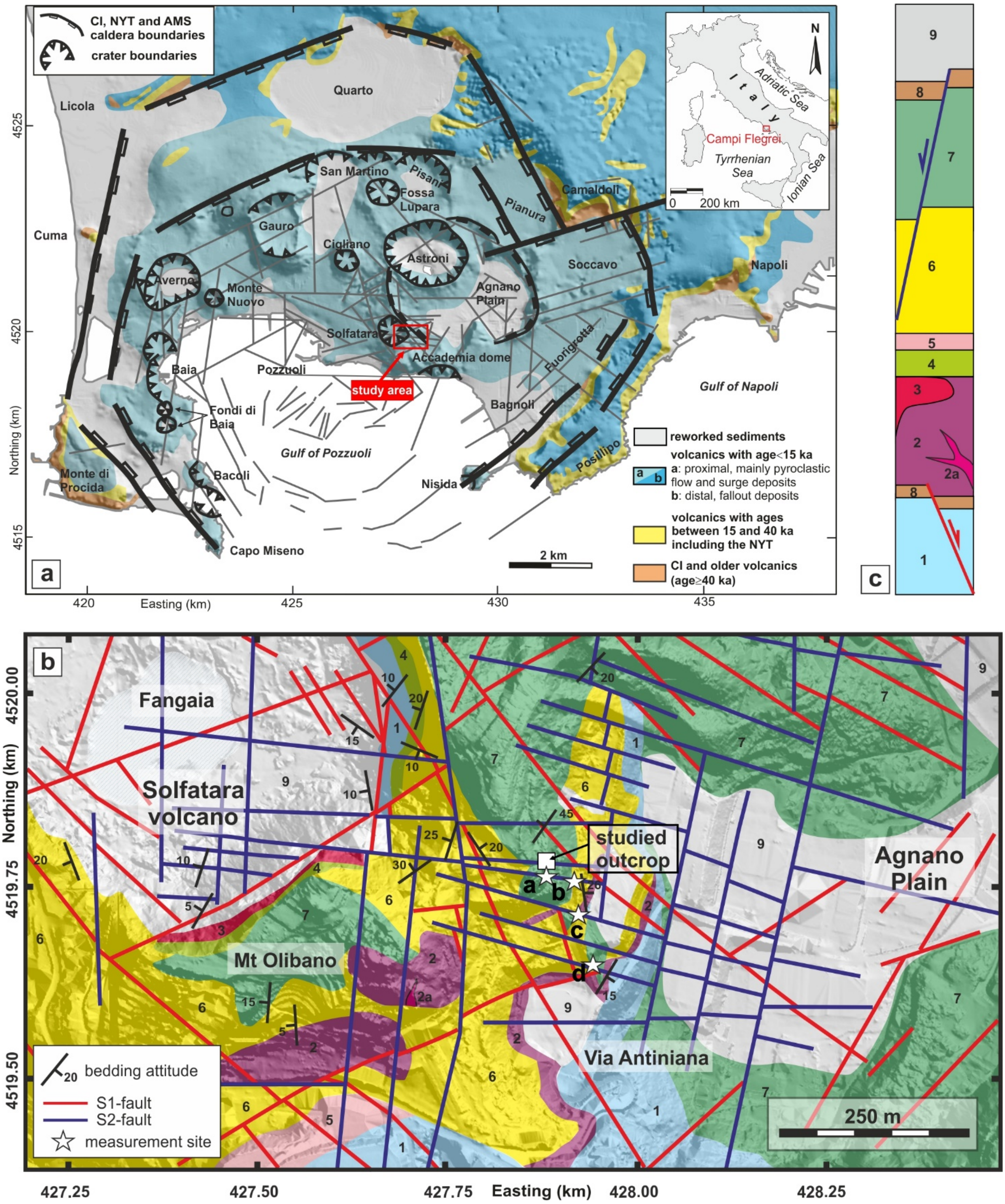


**Figure 1.1.** (a) Geological map of the Campi Flegrei (modified after Isaia et al., 2021). (b) Geological map of southern sector of the Solfatara volcano-Agnano Plain area (modified after Isaia et al., 2021). (c) Stratigraphic log of the study area. 1: Agnano-Monte Spina (AMS); 2: Santa Maria delle Grazie (SMG); 2a: dike; 3: Olibano Dome; 4: Olibano tephra (OLI); 5: Accademia Dome; 6: Solfatara (SOL); 7: Astroni (AST); 8: paleosol; 9: Recent deposits.

The analyzed fault array is situated on the western side of the Agnano Plain (**Fig. 1.1b**), known for its intricate fault pattern, which is composed primarily of two fault systems: S1 and S2. System S1 involves NW-SE and NE-SW high-angle normal faults associated with the AMS caldera, intersecting all volcanic successions up to the AMS tephra (Isaia et al., 2021). Within the Agnano Plain, the younger volcanic sequences of Santa Maria delle Grazie (SGM), Olibano (OLI), Solfatara, and Astroni tephra overlay the S1 system, constituting the host for the subsequent fault system, S2. The S2 system comprises predominantly ESE-WNW and secondary NNE-SSW high-angle normal faults, which Vitale et al. (2019) linked to unrest activities preceding the Monte Nuovo eruption.

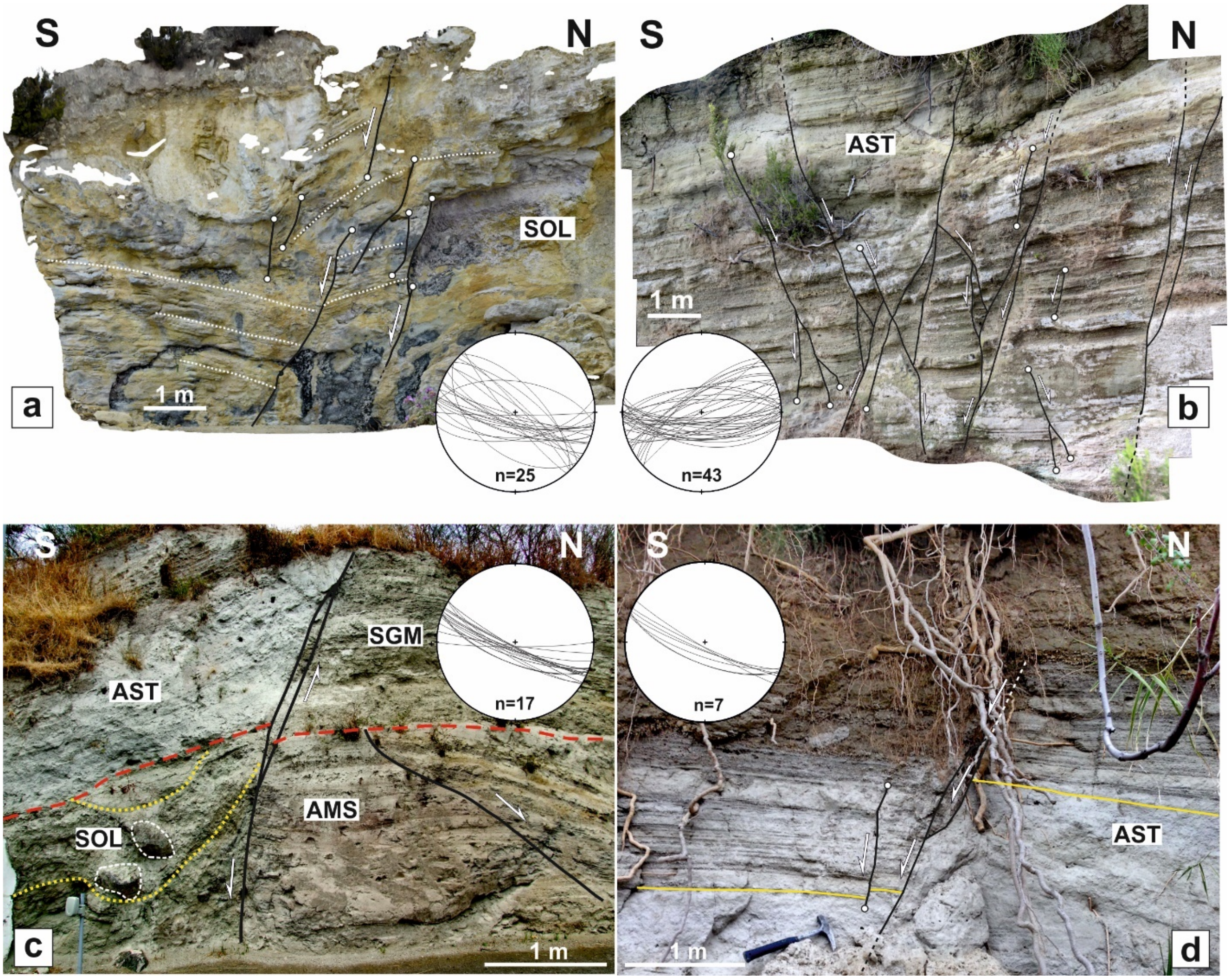


**Figure 1.2.** (a-d) Field photos of the WNW-ESE fault system exposed in the analyzed area with stereographic projections (equiareal net, lower hemisphere) of the measured fault planes. With circles indicate faults tip points. The sites (a-d) are shown in the map of **Figure 1.1b**.

**Figure 1.2** exhibits multiple outcrops vividly displaying ca. E-W normal faults belonging to the S2 fault system, crossing the younger succession with diverse displacements from a few centimetres to several meters. This fault array, part of the S2 system, appears within an inactive potassium alum quarry, a site currently witnessing volcanic degassing and shallow seismic activity (**Fig. 1.3**; Troiano et al., 2019; Isaia et al., 2021). Vertically displayed on a roughly 4-meter high, N-S oriented cliff, the studied fault array presents a well-layered pyroclastic succession of the Astroni unit (Isaia et al., 2004; 2015; **Fig. 1.3**). The Astroni tephra at this outcrop showcases varying hydrothermal alterations, comprising alternating layers of cm- to dm-thick pumice lapilli and ash. Local features include bedforms like dunes (**Fig. 1.3**), resulting from pyroclastic density current deposition and emplacement.

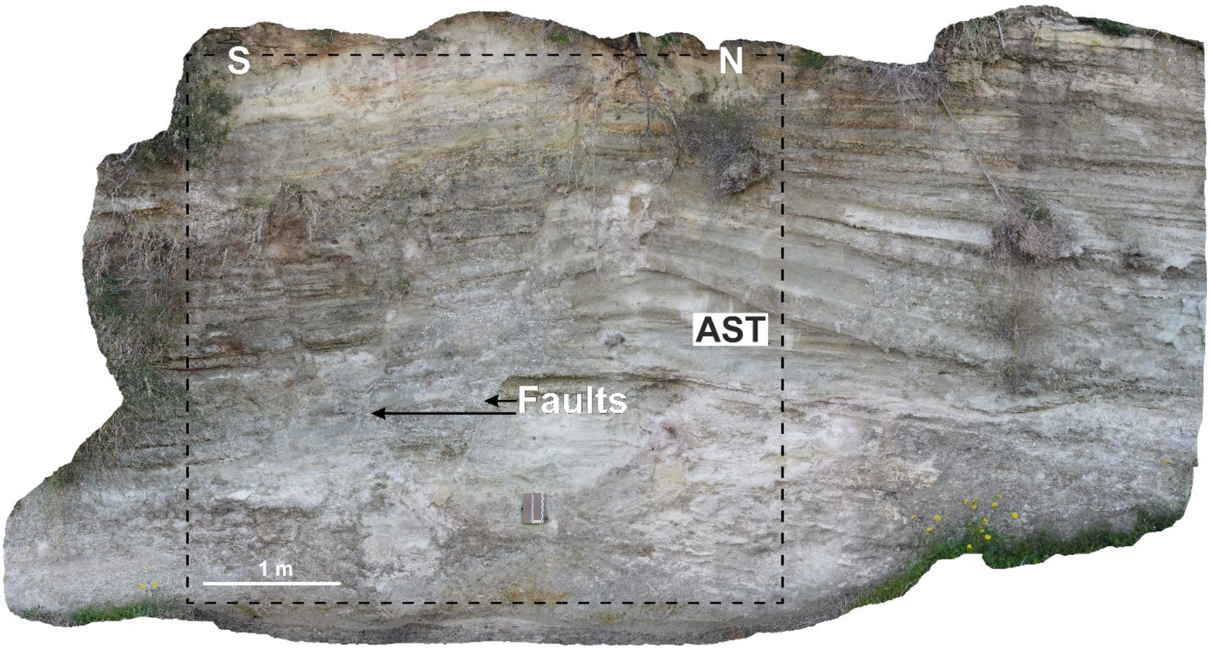


**Figure 1.3.** Orthomosaic of the analyzed outcrop (the site is shown in **Figure 1.1**).

### 1.3 Virtual outcrop modelling

The fault array under investigation was subjected to structural analyses, employing a comprehensive approach encompassing fieldwork and the utilization of an orthophotograph obtained from a virtual outcrop model (**Figs. 1.3** and **1.4**). The creation of this model involved employing structure from motion-multi-view stereophotogrammetric techniques (Westoby et al., 2012; James et al., 2012) through the Agisoft Metashape software (version 1.5.1) using digital photos captured by a drone. A total of 46 images were collected utilizing a DJI Mavic Air 2 UAS equipped with a 1/2" CMOS 12 MP sensor and a 4.5mm (24 mm equivalent) focal length lens. These images were acquired perpendicularly to the outcrop from a distance of 2 meters, ensuring a front and side overlap of at least 90%. Leveraging an optimal exposition to the satellite constellation, we relied on the UAS positioning system to accurately determine camera locations, resulting in less than 1 cm error on the Z, X, and Y axes. Consequently, the orthophotograph used for structural analyses boasts a resolution of 0.5 mm per pixel, ensuring a detailed and precise examination of the fault array's structural characteristics.

### 1.4 Fault zone structure and throw analysis

The structural analyses commenced by characterizing the fault array, initially focusing on identifying its constituent faults, determining their movement senses, and directly measuring their orientation in the field. The exceptional exposure of stratified deposits facilitated the identification of 9 dislocated thinly-bedded stratigraphic horizons throughout the studied fault array distributed across the area (**Fig. 1.4**). These stratigraphic layers served as crucial markers for precisely defining the throw distribution along faults. Detailed throw profiles were meticulously constructed to assess the variability of throw values along individual fault segments (e.g., Nicol et al., 2016; Camanni et al., 2019, 2021; Delogkos et al., 2020). These profiles depicted the throw value for each layer against the distance, measured parallel to the individual fault traces, extending from an origin point to the mid-point between the footwall and hanging wall cut-offs of that specific layer. This method provided a comprehensive understanding of the fault displacement distribution across the studied area.

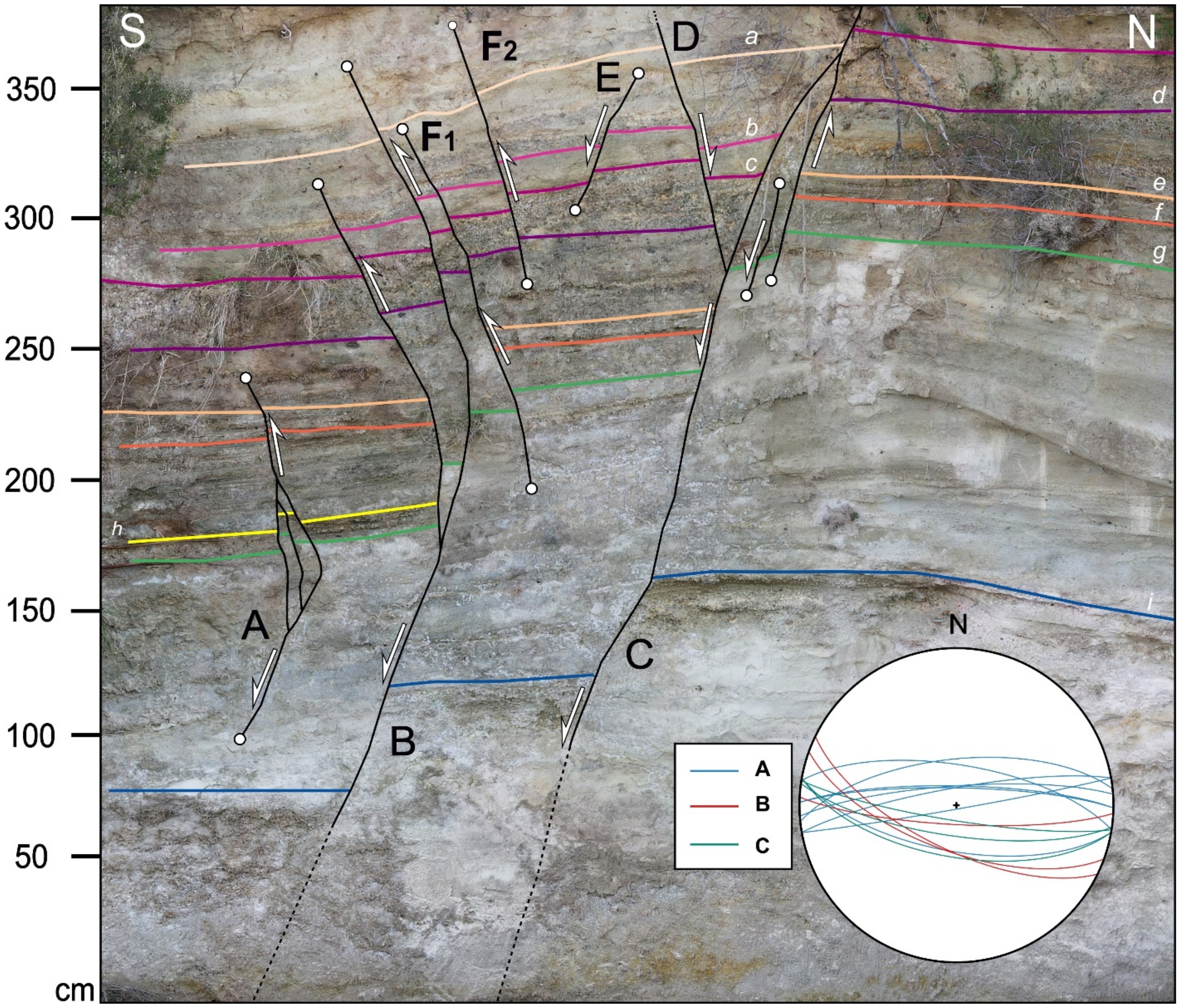


**Figure 1.4.** Line drawing of the analyzed fault array with Stereographic projection (equiareal net, lower hemisphere) of the measured fault planes.

### 1.4.1 Description of the fault array

The examined outcrop exhibits a diverse array of faults encompassing both normal and reverse movements, collectively causing downthrows of the pyroclastic beds towards the south (**Fig. 1.4**). These faults primarily strike in an approximate E-W direction and possess steep dips, observed both to the south and north, as indicated in the stereographic projection depicted in **Fig. 1.4.**

Faults B and C exhibit a southward dip toward the lower section of the outcrop and demonstrate a normal sense of movement. However, fault B undergoes an upward curvature in the upper section and branches into two north-dipping segments, each displaying a reverse sense of movement.

Similarly, fault A, positioned as an isolated segment southward of fault B, presents a convex northward curvature. This fault showcases both reverse and normal senses of movement in its upper and lower portions, respectively.

The uppermost part of the outcrop features three faults: two north-dipping faults (F1 and F2) demonstrating a reverse sense of movement and one south-dipping normal fault (E). Lastly, fault C adjoins the north-dipping normal fault D in its upper region. This intricate fault arrangement contributes to the overall structural complexity observed within the outcrop.

### 1.4.2 Throw analysis

The throw profiles outlined in **Figure 1.5** demonstrate that faults B and C exhibit the most substantial throws within the array, although both showcase notable variations in throw along their dips. Fault B reveals an overall decline in throw from approximately 40 cm at the lower end of data extent across the horizon “i” to 0 cm at its uppermost point(s). This reduction is not consistent but instead reveals a lower gradient in the outcrop bottom part, transitioning to a steeper gradient in its upper section, notably marked near the horizon “d”.

Conversely, fault C displays higher throw values in its upper segment, with the maximum throw reaching approximately 60 cm across the horizon “c”, gradually decreasing to around 40 cm at the lower end of data across the horizon “I”.

Faults A, F1, F2, and E exhibit full-extent cropping from their upper to lower tip points. Their maximum throw values range between approximately 5 cm and 10 cm. Maximum values are centrally positioned along faults A and E and closer to the lower tip points of faults F1 and F2. This variation results in bell-shaped and asymmetric throw profiles for faults A and E and F1 and F2, respectively. Lastly, fault D showcases a maximum throw of roughly 8 cm. The data suggests that the throw on fault D decreases to 0 cm in correspondence with the juncture point with fault C. However, due to data resolution limitations, precise estimation of the throw at this location remains challenging.

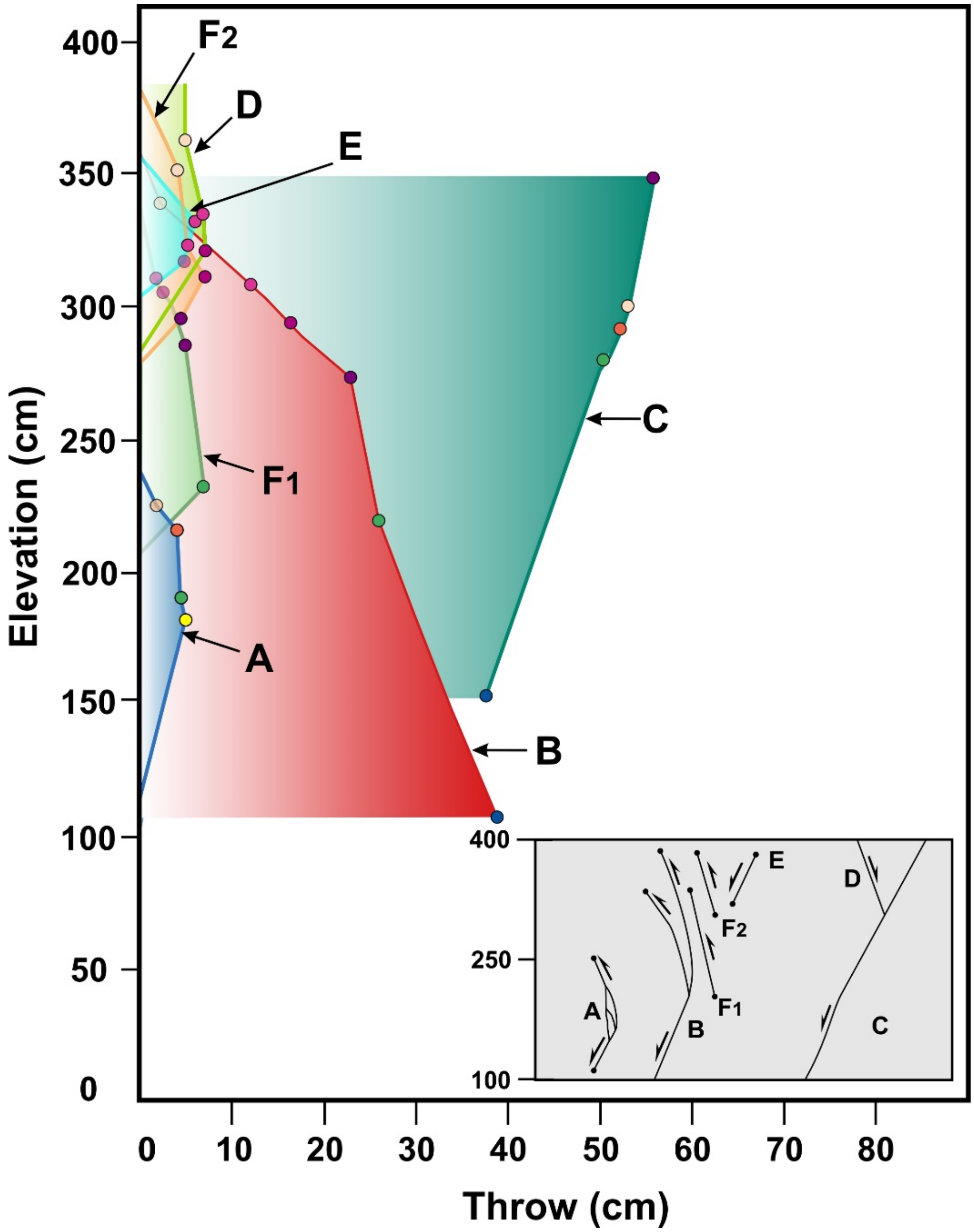


**Figure 1.5.** Throw diagram for the different faults constituting the array. Circles in the diagram are coloured as the same as the dislocated layer to which they referred (see **Figure 1.4**).

### 1.5. Kinematic coherence of the fault array

Faults rarely exist in isolation but instead form arrays of fault segments, each contributing to accommodating a portion of displacement (Childs et al., 1996, 2009, 2017; Delogkos et al., 2020; Kristensen et al., 2008; Marchal et al., 2003; Peacock, 2002; Walsh and Watterson, 1989; Walsh et al., 2003). Notably, it has been widely observed, particularly within normal fault systems, that throws accommodated by individual fault segments often amalgamate into a relatively smooth total throw profile resembling that of an individual fault (e.g., Childs et al., 2017; Jackson and Rotevatn, 2013; Nicol et al., 2010, 2016; Walsh et al., 2003; Camanni et al., 2021). These observations have led to the concept of "kinematic coherence" (e.g., Childs et al., 2017; Walsh and Watterson, 1991), suggesting the essentiality of each individual fault segment for the fault system kinematics.

In subsequent discussions, faults A-B-F1-F2-E are delineated as hanging wall faults, while fault C is identified as the footwall fault, based on their respective locations within the hanging wall and footwall of a relatively undeformed rock volume (**Fig. 1.4**). The collective throw of all hanging wall faults showcases an upward decreasing trend (**Fig. 1.6**), akin to the individual fault B profile (**Fig. 1.5**), albeit appearing smoother overall. This indicates the kinematic coherence of faults A-F1-F2-E with fault B. These faults exhibit both normal and reverse movements, suggesting their joint action in down throwing the succession southward. Intriguingly, normal and reverse faults coexist within an area where overall throw on the hanging wall faults decreases, resembling the horse-tail geometries described at the terminations of strike-slip faults (e.g., Kim et al., 2004).

Upon detailed examination of throw distribution on the hanging wall faults and fault C, a symmetrical relationship emerges: while the hanging wall faults display an increasing throw downward, fault C exhibits an increasing throw upward (**Fig. 1.6**). These cumulative throws approximate a relatively constant aggregate of about 80 cm, marginally decreasing upward to approximately 65 cm (**Fig. 1.6**). This implies displacement transfer processes between hanging wall faults and fault C, defining the latter as the bounding faults of a relay zone (e.g., Delogkos et al., 2020; Camanni et al., 2019; Childs et al., 1996; Huggins et al., 1995; Nicol et al., 2020; Peacock and Sanderson, 1991, 1994; Roche et al., 2020, 2021). Finally, the increasing throw upward in fault C and the decreasing throw downward in the hanging wall faults suggest the relay zone's geometric characterization as a dip, contractional relay zone (following the concepts by Camanni et al., 2019; Roche et al., 2021).

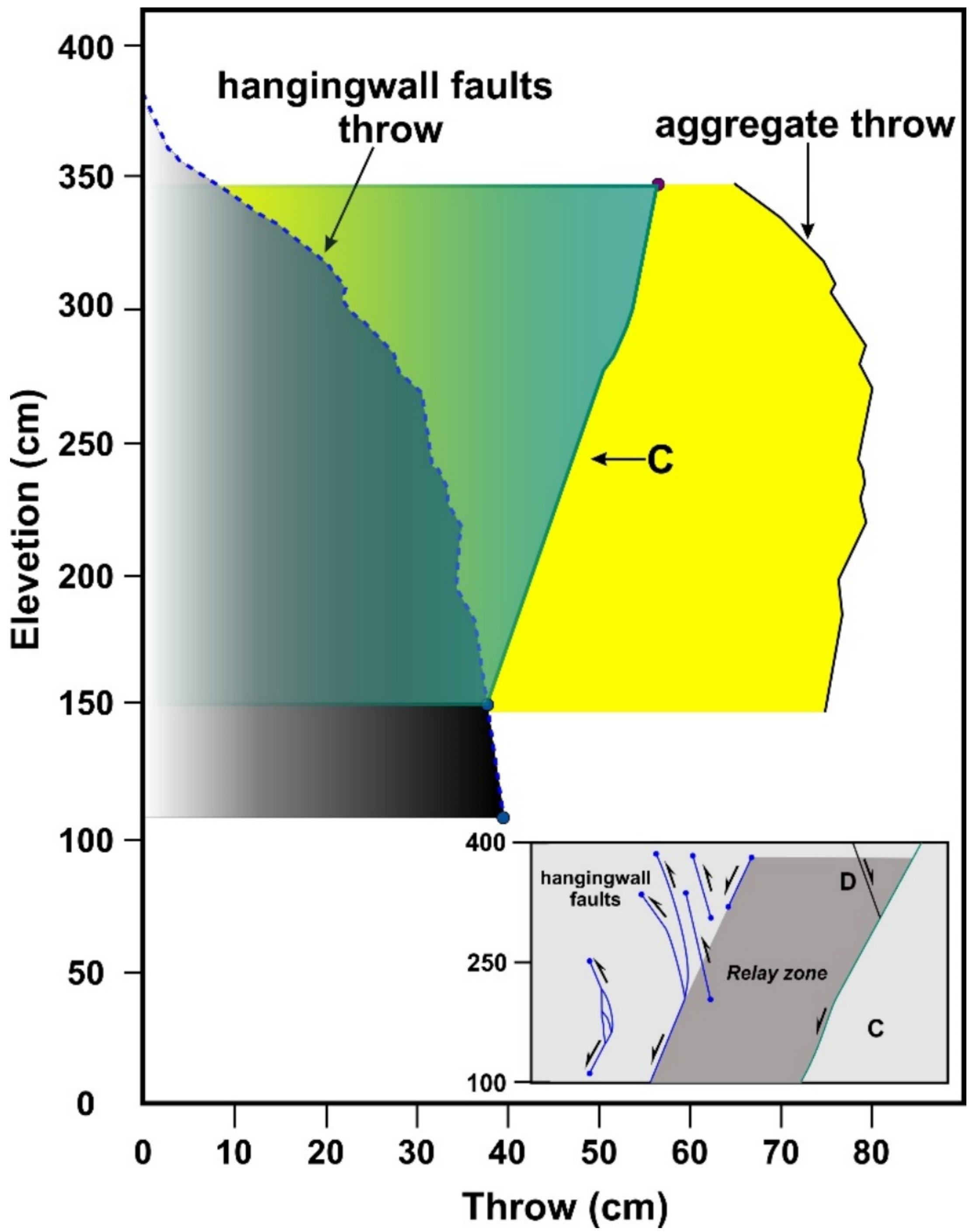


**Figure 1.6.** Aggregate throw diagram showing strain distribution of hanging wall faults and the footwall fault "C". The opposite throw pattern of these two fault systems sums in a rather constant aggregate distribution. This is characteristic of relay zones where displacement distribution through the relay zone bounding fault is enhanced. Circles in the diagram are coloured as the same as the dislocated layer to which they referred (see **Figure 1.4**).

## 1.6. The origin of the studied fault array

The findings from this study affirm the "kinematic coherence" observed within the examined fault array, which comprises steeply dipping normal and reverse faults acting collectively to downthrow the bedding southward. This juxtaposition of steeply-dipping normal and reverse faults, seen in volcanic areas during gravitational collapses (Acocella, 2007; Branney, 1995; Branney and Acocella, 2015; Walker, 1984; Burchardt and Walter, 2010; Kennedy et al., 2004), resembles fault arrays in other non-volcanic settings, such as those formed due to ground subsidence (e.g., sinkholes, Poppe et al., 2015), mining subsidence, or permafrost-type collapses resulting from ice melting (Branney, 1995). Consequently, a plausible explanation for the genesis of the studied fault array is its formation to accommodate a gravitational collapse. The faults within the study area are believed to have facilitated various collapses, including those linked to the AMS caldera (De Vita et al., 1999) and the Solfatara maar-diatreme evolution (Isaia et al., 2015). The ESE-WNW-oriented S2 fault system, housing the analyzed fault array, constitutes the youngest structures within the CFc's central sector and spans the entire area (e.g., Vitale and Isaia, 2014; Isaia et al., 2015; Vitale et al., 2019). These faults cut across older structures associated with the AMS caldera collapse (De Vita et al., 1999), including the S1 fault system depicted in **Figure 1.1a**. The S2 fault system is linked to ground deformation preceding the 1538 CE Monte Nuovo eruption (Vitale et al., 2019; Bevilacqua et al., 2020). In this context, the ESE-WNW faults, responsible for lowering the southern sector of the caldera, are envisioned as part of the subsidence subsequent to the draining of a magma chamber at depth (about 3 km b.s.l.; Macedonio et al., 2014; D'Auria et al., 2015) and the subsequent magma transfer from the CFc central sector to the caldera western side (**Fig. 1.7**), as proposed by Di Vito et al. (2016). The presence of steeply dipping normal and reverse faults within the fault array aligns with this model, reinforcing their gravitational origin. Lastly, there a possibility that the orientation of these gravitational faults was affected by a slight reactivation of previously formed inherited structures from the AMS caldera collapse within the CFc (Natale et al., 2020).

## 1.7 A gravitational origin for the analyzed volcano-tectonic faults

This study presents a structural analysis of a fault array located within the volcanic succession of the Campi Flegrei caldera in southern Italy. The volcanic succession consists of distinct thin layers of ash and pumice, allowing for a meticulous investigation of the throw along the array's various faults. The fault array under scrutiny is situated in an area of the Campi Flegrei impacted by two intersecting normal fault systems. The older fault system (S1), characterized by NW-SE and NE-SW orientations, is associated with the formation of the minor Agnano-Monte Spina caldera. In contrast, the younger fault system (S2) comprises a prevailing E-W direction, cutting across all pre-existing structures. The studied fault array is part of the latter system, featuring steeply dipping faults showing local normal and reverse kinematics. Analysis of throw patterns indicates simultaneous actions of these faults with opposing kinematics, revealing kinematic coherence. These findings align with results obtained from analog and numerical experiments on faults generated by gravitational collapses in volcanic regions. Consequently, it is suggested that the studied fault array results from the subsidence of the central area of the Campi Flegrei caldera, triggered by the historical Monte Nuovo eruption of 1538 CE. The collapse, attributed to the emptying of a magma chamber at the caldera's center and subsequent magma migration to its western side, led to the development of shallow, steeply dipping faults like the ones examined in this study.

This field-based research contributes significantly to understanding the detailed structural attributes of faults involved in gravitational movements across various contexts, not limited to volcanic settings. Elucidating their structure holds substantial implications for evaluating magma and hydrothermal fluid movements, identifying heat flow anomalies, and understanding rock alteration processes.

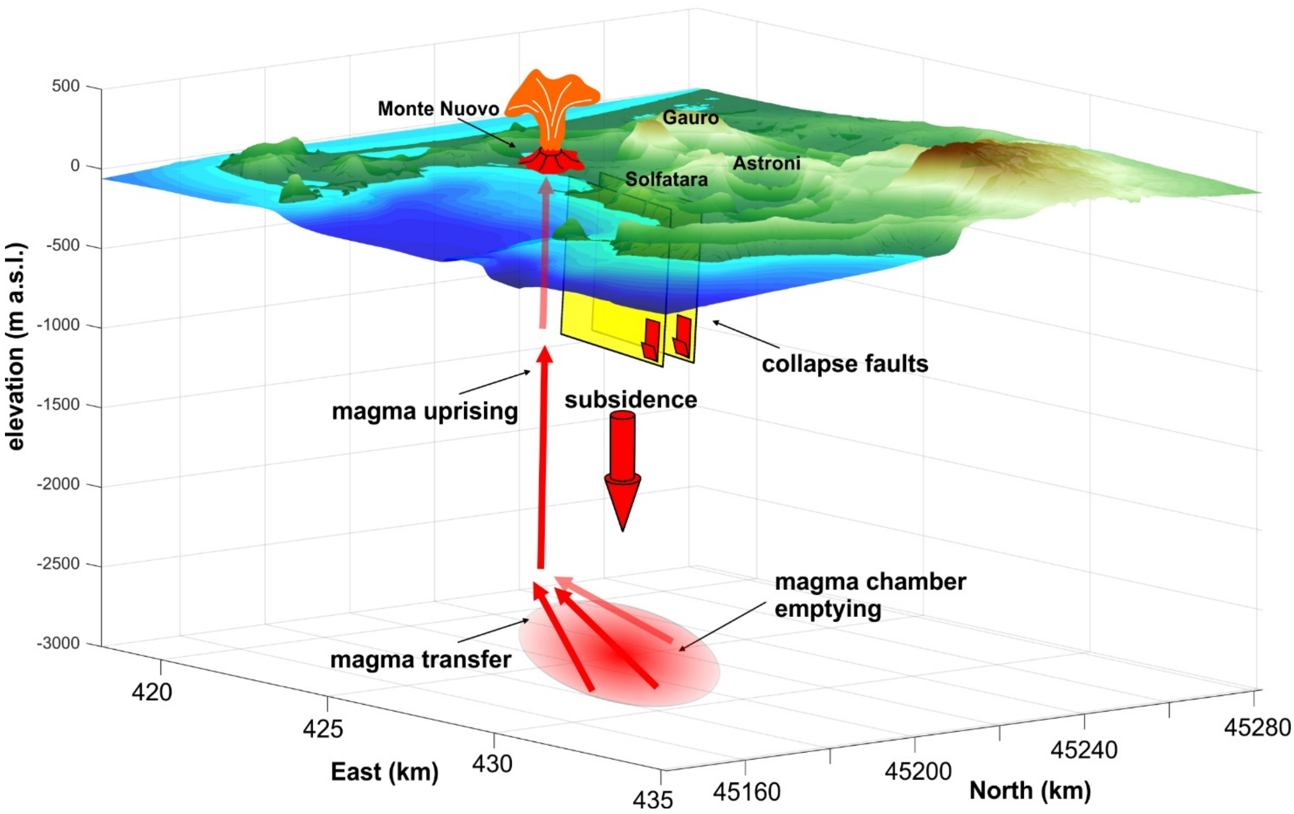


**Figure 1.7.** 3D model of the gravitational collapse faults associated with the subsidence following the magma chamber emptying.

## CHAPTER II

## 2. POLY-DEFORMED FAULT ZONE DEVELOPED WHITIN NORIAN DOLOMITES IN THE SOUTHERN APENNINES

### 2.1 Poly-deformed fault zone

Understanding how heterogeneous rock volumes deform is a crucial aspect of structural geology (Peacock and Mann, 2005; Laubach et al., 2009; Ferrill et al., 2017; Cawood and Bond, 2018). Many studies have explored the relationships between stratigraphic and mechanical anisotropies and strain accommodation mechanisms (Pfiffner, 1993; Erickson, 1996; Shackleton et al., 2005; Ferrill and Morris, 2008; Agosta et al., 2015; Carlini et al., 2019; Oliveira et al., 2022) at the scale of thin section (e.g., Hooker et al., 2013; Tesei et al., 2013; Bullock et al., 2014; Cilona et al., 2014; Wu et al., 2023), outcrop (e.g. Roche et al., 2012; Cawood and Bond, 2018; Ferrill et al., 2021) and whole regions (Pfiffner, 1993; Ferrill and Morris, 2008; Watkins et al., 2015), primarily in extensional (Morris and Ferrill, 2009; Ferrill et al., 2007, 2016; Camanni et al., 2019; Roche et al., 2020, 2021) and compressional tectonic settings (Pfiffner, 1993; Hardy and Finch, 2007; Ferrill et al., 2016; Frehner and Schmid, 2016). Importantly for this work, the mechanical stratigraphy of a layered rock sequence, defined by its mechanical and frictional properties and layer thickness (e.g., Ferrill et al., 2017), has been shown to impact fault nucleation and growth (Childs et al., 1996; Schöpfer et al., 2006; Ferrill and Morris, 2008; Roche et al., 2012; Roche et al., 2021), the 2D and 3D geometry and segmentation of faults (Peacock and Sanderson, 1992; Peacock and Zhang 1993; McGrath and Davison, 1995; Childs et al., 1996, 2009; Rykkelid and Fossen, 2002; Ferrill and Morris, 2003; Schöpfer et al. 2006, 2007; Putz-Perrier and Sanderson, 2008; Morris et al., 2009; Ferrill et al., 2014, 2017; Carlini et al., 2019; Camanni et al., 2019, 2023a, b; Roche et al., 2020, 2021), and strain localization and deformation mechanisms (Willis, 1894; Laubach et al., 2009; Schöpfer et al., 2006; Druguet et al., 2009; Agosta et al., 2015; Jackson and Lewis, 2016; Coleman et al., 2017; Ferrill et al., 2017; Camanni et al., 2021; Cawood and Bond, 2018; Lyu et al., 2022; Oliveira et al., 2022).

Significantly, mechanical anisotropies can also develop in response to strain accommodation processes along faults within the upper crust, and these anisotropies can overprint the primary stratigraphic layering. For instance, it is well known that fault nucleation and progressive growth may lead to the juxtaposition of variably deformed fault-related rocks, such as cataclasite, breccia, and gouge (Sibson, 1977; Eichhubl et al., 2009; Faulkner et al., 2010; Tartaglia et al., 2020; Cardello et al., 2024). Frequently, these fault rocks are defined by laterally juxtaposed, tabular rock panels sub-parallel to the fault (Childs et al., 2009; Agosta et al., 2015; Ferraro et al., 2018; Torabi et al., 2020) and are characterized by different petrophysical properties including, among others, the uniaxial compressive strength (UCS), particle size distribution (PSD), porosity, pores geometry and type, and permeability (Sibson, 1977; Mooney and Ginzburg, 1986; Morrow and Lockner, 2001; Rawling et al., 2001; Sperrevik et al., 2002; Billi and Storti, 2004; Agosta et al., 2006; Agosta et al., 2007; Fredman et al., 2007; Collettini et al., 2009; Balsamo and Storti, 2010; Jeanne et a., 2012; Torabi et al., 2013, 2018; Michie and Haines, 2016; Ferraro et al., 2020; Tomassi et al., 2023). Therefore, these fault rock units define a mechanical layering that can variously affect the development of successive faults that may cut across it, in a similar fashion to the primary mechanical stratigraphy. However, while the impact of stratigraphic layering on deformation patterns and mechanisms is well explored in the literature, how inherited tectonic anisotropies associated with fault rock development affect the deformation of a successive faulting event is less described.

This study addresses this and aims to describe how an inherited, layered brittle fault zone in dolostones in the Matese massif (southern Apennines, Italy) influenced the geometry and the deformation mechanisms of a subsequent, superposed fault zone. In detail, following previous studies on mechanical stratigraphy (Shackleton et al., 2005; Cooke et al., 2006; Laubach et al., 2009; Agosta et al., 2015; Guerriero et al., 2013, 2015; Giorgioni et al., 2016; Ferrill et al., 2017), this work aims at characterizing the spatial distribution and the physical and mechanical properties of the inherited layered rocks, such as the fabric, PSD, porosity and the uniaxial compressive strength (UCS), and to investigate how these affect the deformation mechanisms and the geometry of the superposed fault array. An enhanced understanding of this can impact not only knowledge of how faults develop in mechanically layered rocks but, most importantly, also industrial applications dealing with fluid flow in reservoirs faulted in successive deformation events.

### 2.2 Tectonic evolution of the southern Apennines

The study area is located in the western sector of the Matese Massif in the southern Apennines, Italy (**Fig. 2.1**). This orogenic region is characterized by the stacking of various tectonic units. At its summit lie the Ligurian units, oceanic successions (Vitale et al., 2019). Beneath these units, there exists a thrust-sheet wedge, comprising deposits ranging from shallow-water to pelagic basin types. These deposits once formed the continental shelf margin of the Adria Plate and are partially detached from their Paleozoic basement (e.g., Noguera and Rea, 2000; Carminati and Doglioni, 2012; Vitale and Ciarcia, 2013). The Apulian carbonates, which have undergone flexure and burial below the Plio-Quaternary Bradanic foredeep basin, represent the downgoing plate.

### 2.3 Stratigraphic and structural setting of the Matese Massif

The Matese Massif exhibits a Mesozoic-Cenozoic carbonate succession that predates the orogenic activity. This succession is comprised of shallow-water carbonates which transition laterally into margin-slope-basin successions, extending both northward and southward (Iannace et al., 2005a; Vitale and Ciarcia, 2022). Overlying these deposits are Miocene synorogenic rocks, which consist of ramp carbonates, pelagic marlstone, and siliciclastic deposits (Sabbatino et al., 2021).

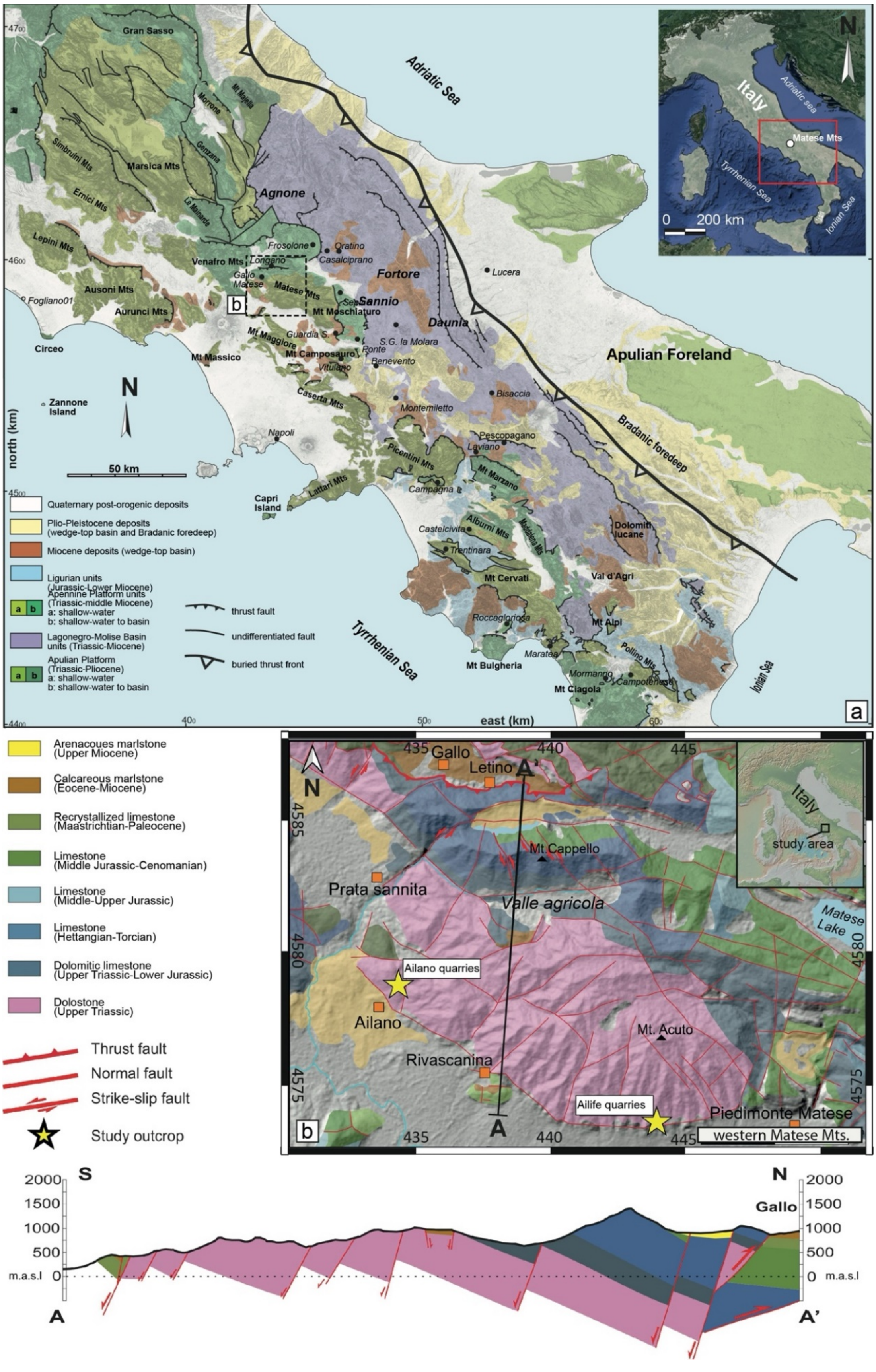


**Figure 2.1.** (a) Geological map of the southern Apennines (from Vitale and Ciarcia, 2013). (b) South-western Matese Massif geological map (modified after Servizio Geologico d'Italia, 1971), cross-section, and location of the study outcrops.

The pre-orogenic succession of the Adria domain underwent significant changes during the Late Triassic-Early Jurassic rifting phase (e.g., Santantonio and Carminati, 2011). This event involved crustal breakup and ocean spreading, reshaping the predominant shallow water sedimentation patterns. It resulted in the development of a complex paleogeography marked by the presence of carbonate platforms, namely the Apennine and Apulian platforms (Mostardini and Merlini, 1986), alongside oceanic domains (Ligurian Ocean) and pelagic areas (Lagonegro-Molise Basin; Scandone, 1967). The Upper Triassic-Lower Jurassic carbonates bear evidence of this rifting phase, showcasing extensive extensional processes. These processes led to the formation of structural depressions, some of which were sites for deep-basin sedimentation (Iannace et al., 2005a, c). Additionally, this period witnessed occurrences of dolomitization events within the carbonates (Bechstädt et al., 1991; Sandulli and Raspini, 2004; Iannace et al., 2011; Ronchi et al., 2012; Barale et al., 2013; Mozafari et al., 2019; Berra et al., 2020; Barale et al., 2021).

# 3. SUCCESSIVE FAULTING EVENTS AND FAULT KINEMATICS

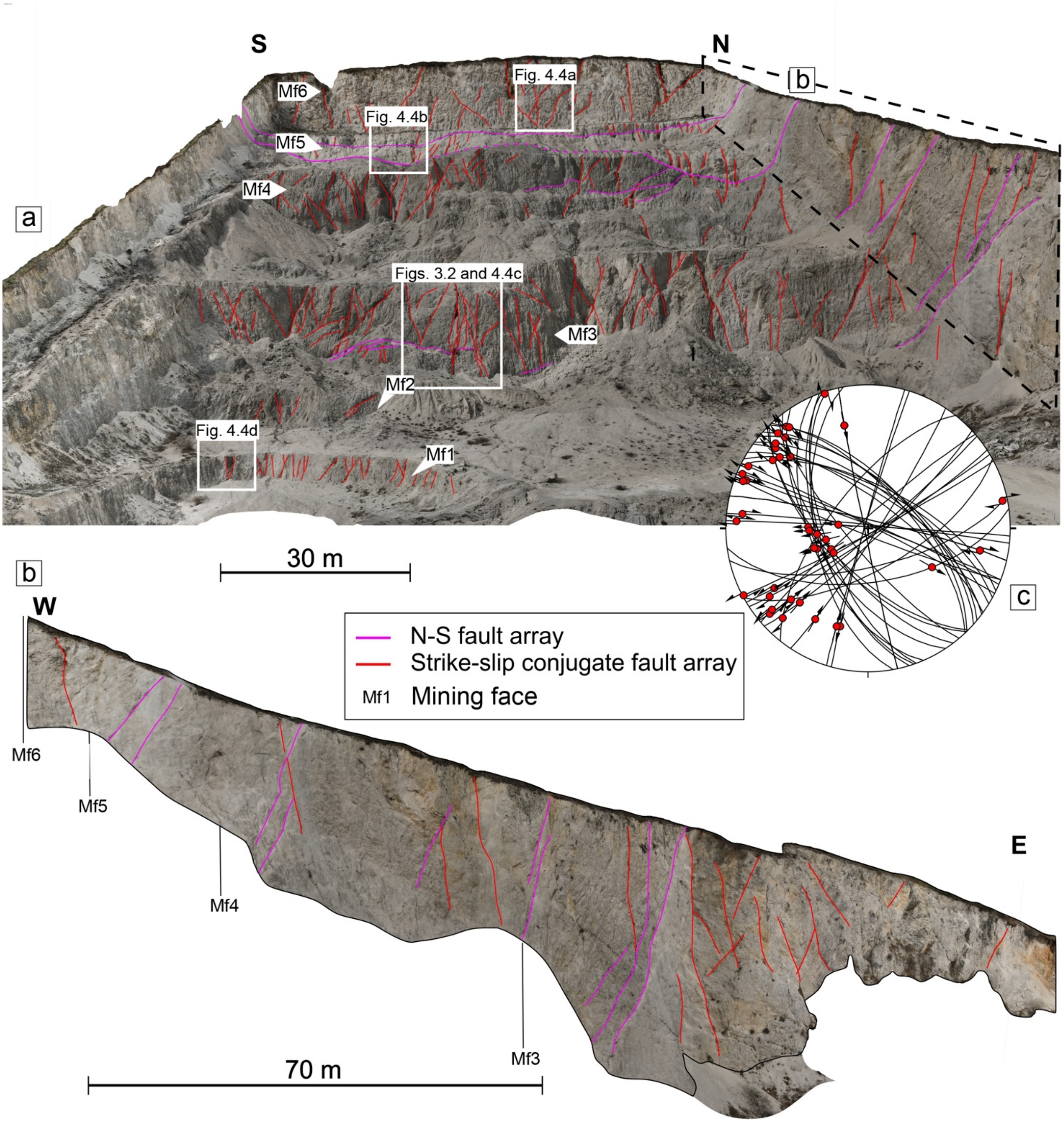


**Figure 3.1.** 3D model of the analyzed quarry and interpretative line drawing of the major fault zones. (a) Westward view of the studied outcrop. (b) Frontal view of the northern quarry slope.

### 3.1 Ailano fault zone

In the dolomite quarry under analysis (**Fig. 3.1**), various fault systems are present, including conjugate sets of normal (designated as system F1) and strike-slip faults (system F2). Observations of cross-cutting relationships reveal that the F1 system is deformed and displaced by the F2 system (**Fig. 3.2a**). The F1 fault system comprises two conjugate sets with an approximate NNW-SSE direction (**Fig. 3.2a, b**). The better-preserved set exhibits a WSW dip, displaying striations, fibers, and steps. Analyzing the PBT plot (**Fig. 3.2b**) reveals an almost vertical P-axis and an extension in the WSW-ENE direction (T-axis), indicating an overall extensional movement of these faults. Throughout the paleostress analyses, the theta angle was maintained at a fixed 30°. Conversely, the F2 fault system comprises two conjugate sets of nearly vertical faults (**Fig. 3.2a, c**). The striking set oriented WNW-ESE (F2a) exhibits dextral, strike-slip kinematics, whereas the SW-NE striking set (F2b) indicates sinistral, strike-slip movements. According to the PBT plot (**Fig. 3.2c**), there is a sub-horizontal NNW-SSE shortening (P-axis) and an extension along the WSW-ENE direction (T-axis). Furthermore, some of the F1 faults display signs of reactivation, characterized by prevalent dextral kinematics (**Fig. 3.2d**). The PBT plot indicates NNW-SSE compression (P-axis) in these cases.

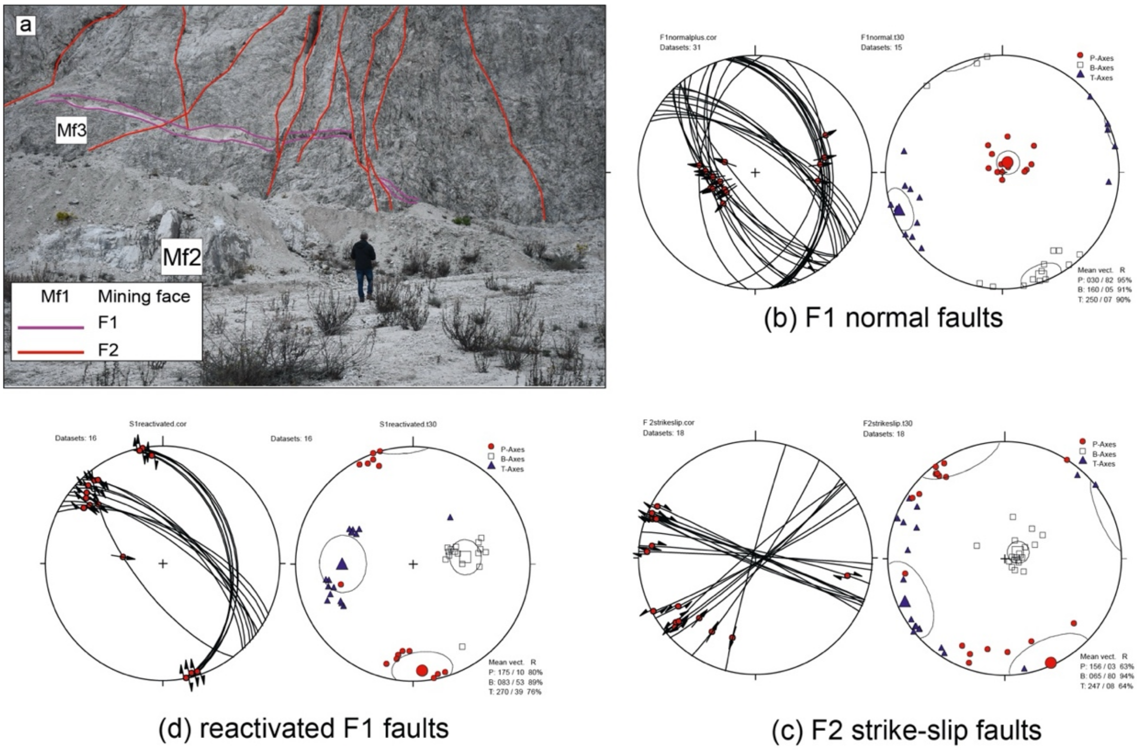


**Figure 3.2.** (a) Panoramic view of a sector of the quarry showing the superposition between F1 and F2 fault systems. Stereographic projections of faults and PBT plots; (b) F1 normal faults; (c) F2 conjugate strike-slip faults; (d) reactivated F1 faults with strike-slip kinematics.

# 6. INTERPLAY OF DOLOMITE TEXTURES AND FAULTING: INSIGHTS FROM MESOZOIC WESTERN ADRIA TECTONIC EVOLUTION

The analysis of fault zones within the Triassic dolomite in the southern Apennines presents an opportunity to shed light on the complex tectonic evolution of the Adria plate, spanning from the Triassic to Quaternary time. This research aimed to discern the intricate interplay between rock fabric changes and the polyphase tectonic evolution of the Norian dolomite. Specifically, this study focused on characterizing Mesozoic normal fault zones and their pivotal role in the evolution of dolomite textures, as well as their influence on subsequent fault zone superposition. The principal outcomes of this research highlight the profound influence of fluid-rock interaction processes and strain accommodation mechanisms in shaping the dynamic evolution of dolomite textures.

CHAPTER III

# 7. FRACTURE PATTERN IN DOLOMITES WITH VARYING GRAIN SIZE DISTRIBUTION

## 7.1 Textural control on carbonate rock strength and fractures patterns

Understanding how rock microstructure influences its strength and deformation features is fundamental in rock mechanics and several other geological disciplines such as structural geology and geotechnics (Robertson, 1955; Smorodinov et al., 1970; Dunn et al., 1973; Hoshino, 1974; Rippa and Vinale, 1983; Kelsall, 1986; Rammamurthy, 1993; Kwasniewski, 1993; Eberhardt et al., 1999; Prikryl, 2001; Sabatakakis et al., 2008; Laubach et al., 2009; Lamarche et al., 2012; Ogata et al., 2017). Many studies have explored this complex interplay between rock textures and brittle deformation through field studies (Pfiffner, 1993; Erickson, 1996; Shackleton et al., 2005; Ferrill and Morris, 2008; Agosta et al., 2015; Carlini et al., 2019; Zhao et al., 2021; Oliveira et al., 2022), rock deformation in the laboratory (Bieniawski, 1968; Hugman and Friedman, 1979; Horii and Nasser, 1985; Menendez et al., 1996; Gupta and Rao, 2000; Zavattieri and Espinosa, 2001; Patersopn and Wong, 2005; Bruning et al., 2018; Li et al., 2020) and numerical modelling (Donzé and Magnier, 1995; Tang et al., 2000; Kaus et al., 2010; Lan et al., 2010; Gao et al., 2016; Yu et al., 2018; Hu et al., 2020; Li et al., 2021; Peng et al., 2022).These studies highlight that the processes of damage initiation, accumulation, and interaction are primarily tensile, with shear mechanisms becoming important only after sufficient tensile damage accumulation and interaction have occurred (Lan et al., 2010 and references therein).

Importantly, for this work, the fracture initiation and propagation mechanisms are influenced by the presence of flaws (Griffith, 1924; Brace, 1961; Olson, 1974; Hugman and Friedman, 1979; Fredrich et al., 1990; Hatzor and Palchik, 1997; Eberhardt et al., 1999) at the scale of rock mass (e.g., bedding, joint and fault) (Hoek and Brown, 1997; Zhao et al., 1999; Larsen et al., 2010; Pollard and Aydin, 1988; Ju and Xing, 2022) and microstructures (e.g., microcracks, void, cleavages and grain boundaries) (Robertson, 1955; Paterson, 1958; Dreyer, 1973; Fahy and Guccione, 1979; Nasseri et al., 2005, 2010; Dai and Xia, 2010; Kataoka et al., 2015; Ju et al., 2022).

Among these different features, grain size is tough to be a fundamental parameter controlling rock mechanical behavior as they represent preexisting defects in the rock microstructure (Nemat-Nasser and Horii, 1982; Ashby and Hallam, 1986; Fredrich et al., 1990; Wong et al., 1996; Hatzor and Palchik, 1997). Grain size has a profound impact on fracture initiation, propagation, and the resulting geometry, ultimately causing material strength degradation and eventual failure (Ju et al., 2022 and references therein). Therefore, the peak strength of rock is observed to decrease inversely with the square root of the grain size (Brace, 1961; Olsson, 1974; Hugman and Friedman, 1979; Fredrich et al., 1990; Wong et al., 1996; Hatzor and Palchik, 1997; Paterson and Wong, 2005).

Experiments on dolostones (Brace, 1964; Hugman and Friedman, 1979; Fredrich et al., 1990; Wong et al., 1996; Hatzor and Palchik, 1998), reported a decrease of the uniaxial compressive strength with increasing grain size, following the prediction of Griffith crack theory (Griffith, 1921). However, the influence of grain size distribution on micro-fractures in dolostone is poorly investigated.

In this section, we present the outcomes of uniaxial compressive strength tests conducted on dolomite samples exhibiting diverse mean grain sizes. These tests were complemented by comprehensive microstructural analyses of failed samples aiming to assess the impact of grain size variations on micro-fracture propagation and the resulting finite fracture patterns. The outcome of this research can be of broad significance for the exploitation and utilization of underground resources and energy, as fracture patterns may impact the fluid flow within dolostones.

### 7.2 Sampling sites

Dolomite is a common mineral constituent within the carbonate successions forming the backbone of the southern Apennine fold and thrust belt (**Fig. 7.1**) (Iannace et al., 2011 and references therein). Following a thorough examination of geological maps, it was established that three distinct dolomites were suitable for sampling: i) well-bedded and graded Norian dolomites at Praia a Mare (**Fig. 7.1a**); ii) syn-tectonic coarse crystalline white sparry void-filling dolomite breccia sourced from the Calcari con Selce Formation (Lagonegro-Molise Basin unit) collected at Tito-Satriano (**Fig. 7.1b**); and iii) dolomitized limestone originating from the Calcare Massiccio Formation gathered at the Circeo Promontory **(Fig. 7.1b)**.

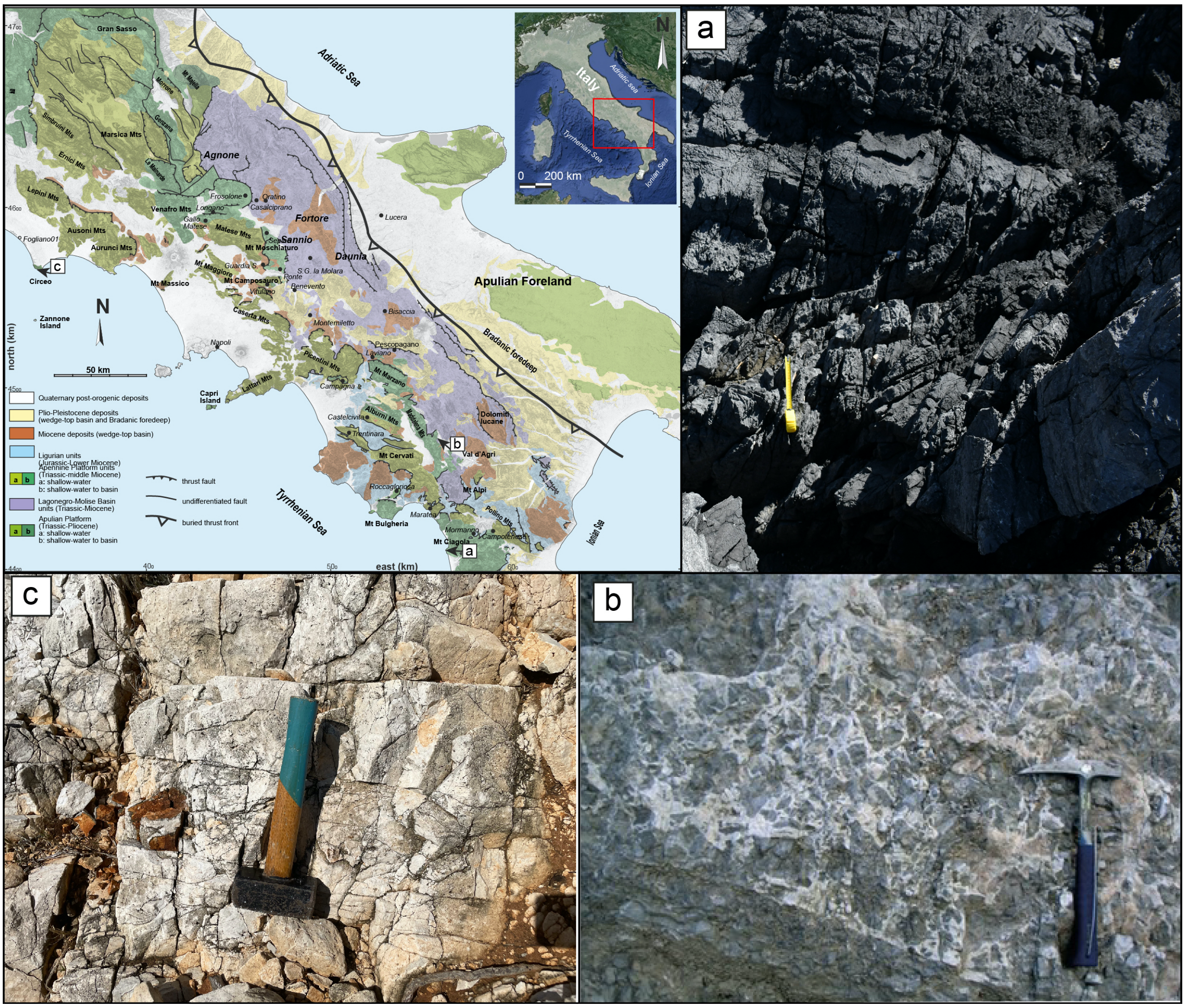


**Figure 7.1.** Geological map of southern Apennines with sampling site locations. (a) Bell bedded-black dololutite found at Praia a Mare. (b) Sy-tectonic dolomite breccias sampled at Tito-Satriano. (c) Dolomitized calcarenites were gathered at Circeo.

### 7.3 Sampling and experimental procedures

One sample for each sampling site was cored from blocks with no apparent signs of weathering and no evidence of macroscopic heterogeneity, such as veins and joints. The lithology and identification of the dolomite samples utilized in the subsequent paragraphs are listed in Table 5.

TABLE 5. DOLOMITE SAMPLES

| Sample location | Texture | Mineralogy | Core size (mm) | ID |
|---|---|---|---|---|
| Praia a Mare | Dololutite | Dolomite | 40.4 x 58.5 | Dolomite 1 |
| Circeo | Dolomitized limestone | Dolomite; subordinate calcite | 36.4 x 49.1 | Dolomite 2 |
| Tito-Satriano | Matrix supported breccia | Dolomite | 36.3 x 43.4 | Dolomite 3 |

Collected samples were tested under uniaxial compression, and the failure mode was classified directly on failed rock samples. Furthermore, to examine fracture patterns at the micro-scale, microstructural and porosity analysis was performed on both the intact samples and the samples after the uniaxial compressive strength (UCS) test.

#### 7.3.1 Petrographic analysis

Six thin sections were obtained from the three groups of dolomites prior and after the UCS test for detailed petrographic analysis. A detailed petrographic analysis was conducted using a Leica DMEP petrographic microscope equipped with a camera. Additionally, SEM-EDS analyses were performed on carbon-coated polished thin sections using a ZEISS Merlin VP Compact. The undeformed dolomite mosaic texture was characterized through the classification proposed by Sibley and Gregg (1984). Optical analysis of the failed rock samples involved examining polished thin sections cut parallel to the core base and orthogonally to the principal fractures. Microfractures were classified in intergranular and intragranular microfractures following the classification scheme in Ju et al., (2022)

### 7.3.2 Mechanical and porosity analysis

The Uniaxial Compressive Strength (UCS) test was conducted on dolomite cylindrical cores, which had their faces previously rectified following the ISRM guidelines (1979) (**Fig. 7.2**).

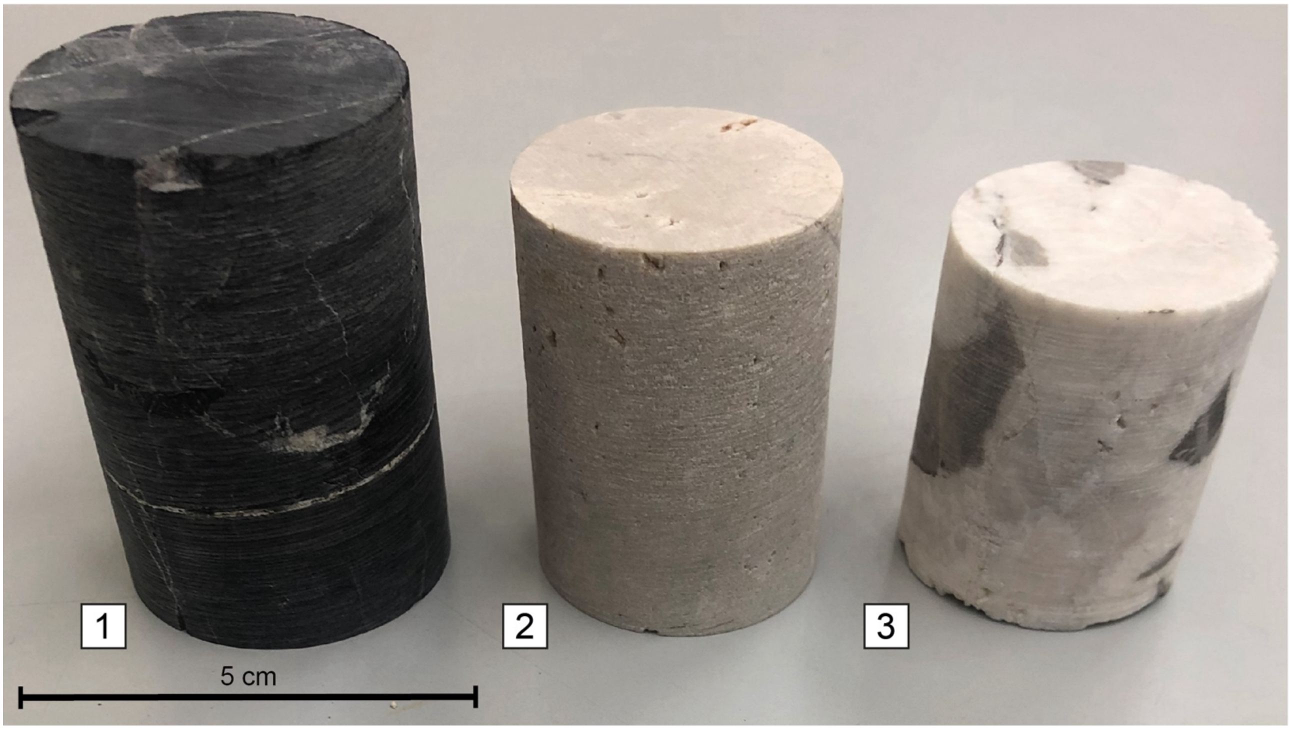


**Figure 7.3.** Rectified cylindrical cores of sampled dolomites: (1) Thinly bedded black dololutites from Praia a Mare. (2) Coarsely grained dolomitized limestones gathered at Circeo promontory. Hydraulic dolomite breccia collected at Tito-Satriano.

These tests were carried out by utilizing the Servo Plus evolution equipment and applying a maximum load of 3000 kN at a constant rate of 0.5 MPa/s until reaching 15% strain post-failure. Laboratory measurements of specific gravity and connected porosity were conducted using a He-pycnometer (Micromeritics Multivolume Pycnometer 1305), providing accuracy between ±0.1 to 0.2%. These measurements were performed for each sample prior to and after failure. By measuring apparent and specific volumes, the porosity of the samples was calculated. Each sample underwent three repetitions of pycnometer measurements to ensure representative values.

### 7.3.3 Failure mode characterization

Failure mode was classified following the scheme proposed by Basu et al., (2013) (**Fig. 7.3**), which reports six varieties of failure mode (i.e., axial splitting, shearing along a single plane, double shear, multiple fracturing, along foliation and Y-shaped) basing on the damage structure pattern.

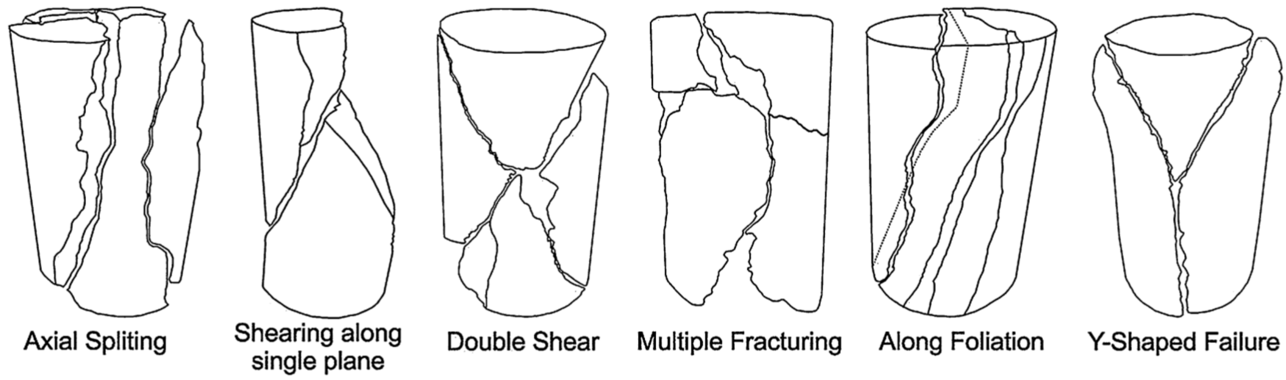


**Figure 7.3.** Conceptual representation of different failure modes under uniaxial compression (from Besu et al., 2013).

# 8. FINAL CONCLUSIONS

In my PhD thesis, I conducted an in-depth examination of fault zone structures in both volcanic and fold-and-thrust belt regions emphasizing their influence on subsurface fluid flow circulation within Chapters I and II. Following, within sections 3 and 4 of Chapter II and in Chapter III, I delved into the exploration of the mutual interconnections between dolomite rock textures and how these textures accommodated deformation processes. These processes are crucial in determining the pathways for fluid flow circulation.

The principal outcomes of these studies reveal that:

- The field-based research, including analysis of throw patterns, contributes significantly to understanding the detailed structural attributes of faults involved in gravitational movements across various contexts, not limited to volcanic settings. Elucidating their structure holds substantial implications for evaluating magma and hydrothermal fluid movements, identifying heat flow anomalies, and understanding rock alteration processes.
- In the Matese massif, the breakup of Pangea continent resulted in fault-controlled hydrothermal dolomitization within fault zones hosted in the Norian dolomite. The extensional tectonics related to the Late Triassic – Early Jurassic rifting induced crustal thinning and cycles of heating pulses due to shallow crustal magmatic intrusions at the borders of the Adria Plate.
- These Mesozoic dolostones were subsequently deformed during the Cenozoic tectonic evolution and formed poly-deformed fault zones. Thus, the role of inherited fault rocks on superposed fault systems was described in terms of meso- and micro-structures, geometries, and deformation mechanisms. Collectively, I found that rock textures (i.e., PSD and porosity) and strength of the inherited fault rock units are the main controls on, respectively, deformation mechanisms (i.e., cataclasis vs. compaction) and geometry (i.e., localized vs. anastomosing) of the superposed fault array.

- Additionally, further investigations were carried out to assess the impact of dolomite textures on compressive strength, failure mode, and microfracture patterns. In general, micromechanical studies highlighted a negative correlation between grain size and unconfined compressive strength (UCS) in dolostones. Furthermore, the tortuosity and density of microfractures appeared to be directly correlated with the mean grain size of the dolomitic texture.

Ultimately, the results obtained from the diverse studies conducted throughout my Ph.D. project can be applied across various geological, engineering, and scientific contexts. Specifically, the emphasized significance of fault zone structures in influencing subsurface fluid circulation, leading to the localization of hydrothermal activity, or accommodating deformation before volcanic eruptions, holds potential applications in refining volcanic hazard assessments and evaluating the hydrothermal fluid movements for the geothermal and exploration industries. At the same time, the envisioned mutual relationships between dolomite rock texture and brittle deformation mechanisms should be considered when characterizing the mechanical and structural behavior of dolostones. This is particularly crucial at both the microstructural scale and fault zone scale, especially in the investigation of poly-deformed fault zones.

## REFERENCES


Abe, S., Van Gent, H., Urai, J. L., 2011. DEM simulation of normal faults in cohesive materials. Tectonophysics, 512(1-4), 12-21.

Ackermann, R. V., Schlische, R. W., Withjack, M. O., 2001. The geometric and statistical evolution of normal fault systems: an experimental study of the effects of mechanical layer thickness on scaling laws: Journal of Structural Geology, v. 23(11), p. 1803-1819.

Acocella, V., 2007. Understanding caldera structure and development: an overview of analogue models compared to natural calderas. Earth Sci. Rev. 85 (3), 125–160. https://doi.org/10.1016/j.earscirev.2007.08.004.

Acocella, V., 2021. Volcano-tectonic processes (Vol. 567). Switzerland: Springer.

Agosta, F., Kirschner, D. L., 2003. Fluid conduits in carbonate-hosted seismogenic normal faults of central Italy. Journal of Geophysical Research: Solid Earth, 108(B4).

Agosta, F., Aydin, A., 2006. Architecture and deformation mechanism of a basin-bounding normal fault in Mesozoic platform carbonates, central Italy: Journal of Structural Geology, v. 28(8), p. 1445-1467.

Agosta, F., Prasad, M., Aydin, A., 2007. Physical properties of carbonate fault rocks, Fucino basin (Central Italy): implications for fault seal in platform carbonates: Geofluids, v. 7(1), p. 19-32.

Agosta, F., Wilson, C., Aydin, A., 2015. The role of mechanical stratigraphy on normal fault growth across a Cretaceous carbonate multi-layer, central Texas (USA): Italian Journal of Geosciences, v. 134(3), p. 423-441.

Alberico, I., Petrosino, P., Lirer, L., 2011. Volcanic hazard and risk assessment in a multi-source volcanic area: the example of Napoli city (Southern Italy). Natural Hazards and Earth System Sciences, 11(4), 1057-1070.

Alneasan, M., Behnia, M., 2021. An experimental investigation on tensile fracturing of brittle rocks by considering the effect of grain size and mineralogical composition. International Journal of Rock Mechanics and Mining Sciences, 137, 104570.

Amoruso, A., Crescentini, L., Berrino, G., 2008. Simultaneous inversion of deformation and gravity changes in a horizontally layered halfspace: evidences for magma intrusion during the 1982–1984 unrest at Campi Flegrei caldera (Italy). Earth Planet Sci. Lett. 272, 181–188. https://doi.org/10.1016/j.epsl.2008.04.040.

Angelier, J., Mechler, P., 1977. Sur une methode graphique de recherche des contraintes principales egalement utilisables en tectonique et en seismologie: la methode des diedres droits: Bulletin de la Société géologique de France, v. 7(6), p. 1309-1318.

Antonellini, M., Aydin, A., 1994. Effect of faulting on fluid flow in porous sandstones: geometry and spatial distribution: AAPG bulletin, v. 79(5), p. 642-671.

Arienzo, I., Carandente, A., Di Renzo, V, Belviso, P., Civetta, L., D'Antonio, M., Orsi, G., 2013. Sr and Nd isotope analysis at the radiogenic isotope laboratory of the National Institute of Geophysics and Volcanology, Naples Section - Vesuvian Observatory. INGV Technical Report No. 260.

Ascione, A., Ciotoli, G., Bigi, S., Buscher, J., Mazzoli, S., Ruggiero, L., Sciarra, A., Tartarello, M. C., Valente, E., 2018. Assessing mantle versus crustal sources for non-volcanic degassing along fault zones in the actively extending southern Apennines mountain belt (Italy). GSA Bulletin, 130(9-10), 1697-1722.

Ashby, M. F. A., Hallam, S. D., 1986. The failure of brittle solids containing small cracks under compressive stress states. Acta metallurgica, 34(3), 497-510.

Aydin, A., 2000. Fractures, faults, and hydrocarbon entrapment, migration and flow. Marine and petroleum geology, 17(7), 797-814.

Balsamo, F., Storti, F., 2010. Grain size and permeability evolution of soft-sediment extensional sub-seismic and seismic fault zones in high-porosity sediments from the Crotone basin, southern Apennines, Italy: Marine and Petroleum Geology, 27(4), 822-837.

Barale, L., Bertok, C., D'Atri, A., Domini, G., Martire, L., Piana, F., 2013. Hydrothermal dolomitization of the carbonate Jurassic succession in the Provençal and Subbriançonnais Domains (Maritime Alps, North-Western Italy). Comptes Rendus Geoscience, 345, 47-53.

Barale, L., Bertok, C., d'Atri, A., Mantovani, A., Martire, L., Agostini, S., Bernasconi, S., M., Ferrando S., 2021. Syn-rift hydrothermal circulation in the Mesozoic carbonates of the western Adriatic continental palaeomargin (Western Southalpine Domain, NW Italy). Basin Research. 33(6), 3045-3076.

Basu, A., Mishra, D. A., Roychowdhury, K., 2013. Rock failure modes under uniaxial compression, Brazilian, and point load tests. Bulletin of Engineering Geology and the environment, 72, 457-475.

Beccaluva, L., Bianchini, G., Coltorti, M., Siena, F., Verde, M., Finetti, I., 2005. Cenozoic tectono-magmatic evolution of the central-western Mediterranean: migration of an arc-interarc basin system and variations in the mode of subduction. Crop Project–Deep Seismic exploration of the Central Mediterranean and Italy. Elsevier Special Volume, 623-640.

Bechstädt, T., Schweizer, T., 1991. The carbonate—clastic cycles of the East-Alpine Raibl group: Result of third-order sea-level fluctuations in the Carnian. Sedimentary Geology. 70(2-4), 241-270.

Benedicto, A., Schultz, R. A., Soliva, R., 2003. Layer thickness and the shape of faults: Geophysical Research Letters, v. 30(20)

Bense, V. F., Gleeson, T., Loveless, S. E., Bour, O., Scibek, J., 2013. Fault zone hydrogeology. Earth-Science Reviews, 127, 171-192.

Berra, F., Jadoul, F., 1996. Norian serpulid and microbial bioconstructions: Implication for the platform evolution in the Lombardy Basin (Southern Alps, Italy). Facies, 35, 143-162.

Berra, F., Galli, M. T., Reghellin, F., Torricelli, S., Fantoni, R., 2009. Stratigraphic evolution of the Triassic–Jurassic succession in the Western Southern Alps (Italy): the record of the two-stage rifting on the distal passive margin of Adria. Basin Research, 21(3), 335-353.

Berra, F., Azmy, K., Della Porta, G., 2020. Stable-isotope and fluid inclusion constraints on the timing of diagenetic events in the dolomitized Dolomia Principale inner platform (Norian, Southern Alps of Italy). Marine and Petroleum Geology. 121, 104615.

Bevilacqua, A., Flandoli, F., Neri, A., Isaia, R., Vitale, S., 2016. Temporal models for the episodic volcanism of Campi Flegrei caldera (Italy) with uncertainty quantification. J. Geophys. Res. Solid Earth 121, 7821–7845. https://doi.org/10.1002/2016JB013171.

Bevilacqua, A., Neri, A., De Martino, P., Isaia, R., Novellino, A., Tramparulo, F.D., Vitale, S., 2020. Radial interpolation of GPS and leveling data of ground deformation in a resurgent caldera: application to Campi Flegrei (Italy). J. Geodes. 94 (2), 24. https://doi.org/10.1007/s00190-020-01355-x.

Bieniawski, Z. T., 1968. The effect of specimen size on compressive strength of coal. International

Journal of Rock Mechanics and Mining Sciences & Geomechanics Abstracts, 5 (4), pp.325-335.

Billi, A., 2005. Grain size distribution and thickness of breccia and gouge zones from thin (< 1 m) strike-slip fault cores in limestone: Journal of Structural Geology, v. 27(10), p. 1823-1837.

Billi, A., 2007. On the extent of size range and power law scaling for particles of natural carbonate fault cores: Journal of Structural Geology, v. 29(9), p. 1512-1521.

Billi, A., 2010. Microtectonics of low-P low-T carbonate fault rocks: Journal of Structural Geology, 32(9), 1392-1402.

Billi, A., Storti, F., 2004. Fractal distribution of particle size in carbonate cataclastic rocks from the core of a regional strike-slip fault zone: Tectonophysics, 384(1-4), 115-128.

Billi, A., Smeraglia, L., Aldega, L., Balsamo, F., Barberio, M. D., Boschi, C., Caracausi, A., Carminati. E., Iannace, A., Mercuri, M., Pizzati, M., Tavani, S., 2023. Dolostone pulverization induced by coseismic rapid decompression of CO2-rich gas in nature (Matese, Apennines, Italy). Earth and Planetary Science Letters, 604, 117996.

Bishop, P., 2007. Long-term landscape evolution: linking tectonics and surface processes. Earth Surface Processes and Landforms: the Journal of the British Geomorphological Research Group, 32(3), 329-365.

Blenkinsop, T. G., 1991. Cataclasis and processes of particle size reduction: Pure and applied geophysics, v. 136, p. 59-86.

Bodvarsson, G. S., Benson, S. M., Witherspoon, P. A., 1982. Theory of the development of geothermal systems charged by vertical faults. Journal of Geophysical Research: Solid Earth, 87(B11), 9317-9328.

Boncio, P., Auciello, E., Amato, V., Aucelli, P., Petrosino, P., Tangari, A. C., Jicha, B. R., 2021. Late Quaternary faulting in southern Matese (central Italy): implications for earthquake potential in the southern Apennines. Solid Earth Discussions, 2021, 1-35.

Bons, P. D., Elburg, M. A., Gomez-Rivas, E., 2012. A review of the formation of tectonic veins and their microstructures. Journal of structural geology, 43, 33-62.

Boschetti, T., Venturelli, G., Toscani, L., Barbieri, M., Mucchino, C., 2005. The Bagni di Lucca thermal waters (Tuscany, Italy): an example of Ca-SO4 waters with high Na/Cl and low Ca/SO4 ratios. Journal of Hydrology, 307(1-4), 270-293.

Brace, W. F., 1961. Dependence of fracture strength of rocks on grain size. In ARMA US Rock Mechanics/Geomechanics Symposium (pp. ARMA-61). ARMA.

Brace, W. F., 1964. Brittle fracture of rocks. In: State of stress in the earth's crust: Proc., International Conference, Santa Monica, 110-178.

Branney, M.J., 1995. Downsag and extension at calderas: new perspectives on collapse geometries from ice-melt, mining, and volcanic subsidence. Bull. Volcanol. 57 (5), 303–318. https://doi.org/10.1007/BF00301290.

Branney, M.J., Acocella, V., 2015. Chapter 16 – calderas. In: Sigurdsson, H. (Ed.), The Encyclopedia of Volcanoes, second ed. Academic Press, pp. 299–315. https://doi.org/10.1016/B978-0-12-385938-9.00016-X.

Bruning, T., Karakus, M., Nguyen, G. D., Goodchild, D., 2018. Experimental study on the damage evolution of brittle rock under triaxial confinement with full circumferential strain control. Rock Mechanics and Rock Engineering, 51, 3321-3341.

Bullock, R. J., De Paola, N., Holdsworth, R. E., Trabucho-Alexandre, J., 2014. Lithological controls on the deformation mechanisms operating within carbonate-hosted faults during the seismic cycle: Journal of Structural Geology, v. 58, p. 22-42.

Burchardt, S., Walter, T.R., 2010. Propagation, linkage, and interaction of caldera ring-faults: comparison between analogue experiments and caldera collapse at Miyakejima, Japan, in 2000. Bull. Volcanol. 72 (3), 297–308. https://doi.org/10.1007/s00445-009-0321-7.

Butler, R. W. H., Mazzoli, S., Corrado, S., De Donatis, M., Di Bucci, D., Gambini, R., Naso, G., Nicolai, C., Scrocca, D., Shiner P., Zucconi, V., 2004. Applying thick-skinned tectonic models to the Apennine thrust belt of Italy—Limitations and implications: AAPG Memoir 82, p. 647-667

Camanni, G., Childs, C., Delogkos, E., Roche, V., Manzocchi, T., Walsh, J., 2023a. The role of antithetic faults in transferring displacement across contractional relay zones on normal faults: Journal of Structural Geology, 168, p. 104827.

Camanni, G., Freda, G., Delogkos, E., Nicol, A., Childs, C., 2023b. 3D geometry and displacement transfer of an oblique relay zone on outcropping normal faults: Journal of Structural Geology, 177, p.105001.

Camanni, G., Roche, V., Childs, C., Manzocchi, T., Walsh, J., Conneally, J., Saqab, M.M., Delogkos, E., 2019. The three-dimensional geometry of relay zones within segmented normal faults. J. Struct. Geol. 129, 103895 https://doi.org/10.1016/j.jsg.2019.103895.

Camanni, G., Vinci, F., Tavani, S., Ferrandino, V., Mazzoli, S., Corradetti, A., Parente, M., Iannace, A., 2021. Fracture density variations within a reservoir-scale normal fault zone: a case study from shallow-water carbonates of southern Italy. J. Struct. Geol.151 https://doi.org/10.1016/j.jsg.2021.104432.

Cardello, G. L., Bernasconi, S. M., Fellin, M. G., Rahn, M., Rosskopf, R., Maden, C., Mancktelow, N. S., 2024. Carbonate deformation through the brittle-ductile transition: The case of the SW Helvetic nappes, Switzerland. Journal of Structural Geology, 105083.

Carlini, M., Viola, G., Mattila, J., Castellucci, L., 2019. The role of mechanical stratigraphy on the refraction of strike-slip faults: Solid Earth, v. 10(1), p. 343-356.

Carminati, E., Aldega, L., Smeraglia, L., Scharf, A., Mattern, F., Albert, R., Gerdes, A., 2020. Tectonic Evolution of the Northern Oman Mountains, Part of the Strait of Hormuz Syntaxis: New Structural and Paleothermal Analyses and U-Pb Dating of Synkinematic Calcite. Tectonics, 39(4), e2019TC005936.

Carminati, E., Doglioni, C., 2012. Alps vs. Apennines: The paradigm of a tectonically asymmetric Earth: Earth-Science Reviews, v. 112(1-2), p. 67-96.

Cassetta, F., Coltorti, M., Ickert, R. B., Bonadiman, C., Giacomoni, P. P., Ntaflos, T., 2018. Intrusion of shoshonitic magmas at shallow crustal depth: T–P path, $H_2O$ estimates, and AFC modeling of the Middle Triassic Predazzo Intrusive Complex (Southern Alps, Italy). Contributions to Mineralogy and Petrology, 173, 1-27.

Cassinis, G., Cortesogno, L., Gaggero, L., Perotti, C. R., Buzzi, L., 2008. Permian to Triassic geodynamic and magmatic evolution of the Brescian Prealps (eastern Lombardy, Italy). Bollettino della Società geologica italiana, 127(3), 501-518.

Cassinis, G., Zezza, U., 1982. Dati geologici e petrografici sui prodotti del magmatismo triassico nelle Prealpi Bresciane. Guida alla geologia del sudalpino centro-orientale; ita; Bologna: Società Geologica Italiana; pp. 157-171;

Cavazza, W., Wezel, F. C., 2003. The Mediterranean region—a geological primer: Episodes Journal of International Geoscience, v. 26(3), p. 160-168.

Cawood, A. J. Bond, C. E., 2018. 3D mechanical stratigraphy of a deformed multi-layer: linking sedimentary architecture and strain partitioning: Journal of Structural Geology, v. 106, p. 54-69.

Chakhmouradian, A. R., Reguir, E. P., Couëslan, C., Yang, P., 2016. Calcite and dolomite in intrusive carbonatites. II. Trace-element variations. Mineralogy and Petrology. 110, 361-377.

Childs, C., Watterson, J., Walsh, J.J., 1995. Fault overlap zones within developing normal fault systems. J. Geol. Soc. 152 (3), 535–549. https://doi.org/10.1144/gsjgs.152.3.0535.

Childs, C., Nicol, A., Walsh, J.J., Watterson, J., 1996. Growth of vertically segmented normal faults. J. Struct. Geol. 18 (12), 1389–1397. https://doi.org/10.1016/S0191-8141(96)00060-0.

Childs, C., Manzocchi, T., Walsh, J.J., Bonson, C.G., Nicol, A., Schöpfer, M.P.J., 2009. A geometric model of fault zone and fault rock thickness variations. J. Struct. Geol. 31 (2), 117–127. https://doi.org/10.1016/j.jsg.2008.08.009.

Childs, C., Holdsworth, R.E., Jackson, C.A.-L., Manzocchi, T., Walsh, J.J., Yielding, G., 2017. Introduction to the geometry and growth of normal faults. Geol. Soc.London. Special Publ 439 (1), 1–9. https://doi.org/10.1144/SP439.24.

Cilona, A., 2019. A Review of Deformation Bands in Carbonates. In Fifth International Conference on Fault and Top Seals: EAGE Publications BV, v. 2019(1), p. 1-5.

Cilona, A., Baud, P., Tondi, E., Agosta, F., Vinciguerra, S., Rustichelli, A., Spiers, C. J., 2012. Deformation bands in porous carbonate grainstones: Field and laboratory observations: Journal of Structural Geology, v. 45, p. 137-157.

Cilona, A., Faulkner, D. R., Tondi, E., Agosta, F., Mancini, L., Rustichelli, A., Baud, P., Vinciguerra, S., 2014. The effects of rock heterogeneity on compaction localization in porous carbonates: Journal of Structural Geology, v. 67, p. 75-93.

Cinque, A., Patacca, E., Scandone, P., Tozzi, M., 1993. Quaternary kinematic evolution of the Southern Apennines. Relationships between surface geological features and deep lithospheric structures. ANNALI DI GEOFISICA, 36(2).

Cioppa, M. T., Al-Aasm, I. S., Symons, D. T. A., Gillen, K. P., 2003. Dating penecontemporaneous dolomitization in carbonate reservoirs: Paleomagnetic, petrographic, and geochemical constraints. AAPG bulletin, 87(1), 71-88.

Climaco, A., Boni, M., Iannace, A., Zamparelli, V., 1997. Platform margins, microbial/serpulids bioconstructions and slope-to-basin sediments in the Upper Triassic of the 'Verbicaro Unit' (Lucania and Calabria, Southern Italy). Facies, 36, 37-56.

Cole, J.W., Milner, D.M., Spinks, K.D., 2005. Calderas and caldera structures: a review. Earth Sci. Rev. 69 (1), 1–26. https://doi.org/10.1016/j.earscirev.2004.06.004.

Coleman, A. J., Jackson, C. A. L., Duffy, O. B., 2017. Balancing sub-and supra-salt strain in salt-influenced rifts: Implications for extension estimates: Journal of Structural Geology, v. 102, p. 208-225.

Collettini, C., Niemeijer, A., Viti, C., Marone, C., 2009. Fault zone fabric and fault weakness: Nature, 462(7275), 907-910.

Cooke, M. L., Simo, J. A., Underwood, C. A., Rijken, P., 2006. Mechanical stratigraphic controls on fracture patterns within carbonates and implications for groundwater flow: Sedimentary Geology, v. 184(3-4), p. 225-239.

Corazzato, C., Tibaldi, A., 2006. Fracture control on type, morphology and distribution of parasitic volcanic cones: an example from Mt. Etna, Italy. Journal of Volcanology and Geothermal Research, 158(1-2), 177-194.

Croizé, D., Ehrenberg, S. N., Bjørlykke, K., Renard, F., Jahren, J. 2010. Petrophysical properties of bioclastic platform carbonates: implications for porosity controls during burial: Marine and Petroleum Geology, v. 27(8), p. 1765-1774.

Curzi, M., Cipriani, A., Aldega, L., Billi, A., Carminati, E., Van der Lelij, R., Vignaroli, G., Viola, G., 2024. Architecture and permeability structure of the Sibillini Mts. Thrust and influence upon recent, extension-related seismicity in the central Apennines (Italy) through fault-valve behavior. GSA Bulletin. 136(1-2), 3-26. doi: https://doi.org/10.1130/B36616.1

D'Auria, L., Pepe, S., Castaldo, R., Giudicepietro, F., Macedonio, G., Ricciolino, P., Tizzani, P., Casu, F., Lanari, R., Manzo, M., Martini, M., Sansosti, E., Zinno, I., 2015. Magma injection beneath the urban area of Naples: a new mechanism for the 2012-2013 volcanic unrest at Campi Flegrei caldera. Sci. Rep. 5 https://doi.org/10.1038/srep13100.

Dahlgren, S., Bogoch, R., Magaritz, M., Michard, A., 1993. Hydrothermal dolomite marbles associated with charnockitic magmatism in the Proterozoic Bamble Shear Belt, south Norway. Contributions to Mineralogy and Petrology. 113, 394-409.

Dai, F., Xia, K., 2010. Loading rate dependence of tensile strength anisotropy of Barre granite. Pure and applied geophysics, 167, 1419-1432.

Davies, G. R., Smith, L. B., 2006. Structurally controlled hydrothermal dolomite reservoir facies: An overview. AAPG bulletin. 90(11), 1641-1690..

De Corso, S., Scrocca, D., Tozzi, M., 1998. Geologia dell'Anticlinale del Matese e implicazioni per la tettonica dell'Appennino molisano. Boll. Soc. Geol. It., 117, 419-441.

De Min, A., Velicogna, M., Ziberna, L., Chiaradia, M., Alberti, A., Marzoli, A., 2020. Triassic magmatism in the European Southern Alps as an early phase of Pangea break-up. Geological Magazine, 157(11), 1800-1822.

De Vita, S., Orsi, G., Civetta, L., Carandente, A., D'Antonio, M., Deino, A., Southon, J., 1999. The Agnano–Monte Spina eruption (4100 years BP) in the restless Campi Flegrei caldera (Italy). J. Volcanol. Geoth. Res. 91 (2–4), 269–301. https://doi.org/10.1016/S0377-0273(99)00039-6.

Deino, A.L., Orsi, G., de Vita, S., Piochi, M., 2004. The age of the Neapolitan Yellow Tuff caldera-forming eruption (Campi Flegrei caldera – Italy) assessed by 40Ar/39Ar dating method. J. Volcanol. Geoth. Res. 133 (1), 157–170. https://doi.org/10.1016/S0377-0273(03)00396-2.

Delogkos, E., Manzocchi, T., Childs, C., Camanni, G., Roche, V., 2020. The 3D structure of a normal fault from multiple outcrop observations. J. Struct. Geol. 136, 104009 https://doi.org/10.1016/j.jsg.2020.104009.

Dempsey, D., Ellis, S., Archer, R., Rowland, J., 2012. Energetics of normal earthquakes on dip-slip faults: Geology, v. 40(3), p. 279-282.

Dholakia, S. K., Aydin, A., Pollard, D. D., Zoback, M. D., 1998. Fault-controlled hydrocarbon pathways in the Monterey Formation, California. AAPG bulletin, 82(8), 1551-1574.

Di Vito, M.A., Acocella, V., Aiello, G., Barra, D., Battaglia, M., Carandente, A., Del Gaudio, C., de Vita, S., Ricciardi, G.P., Ricco, C., Scandone, R., Terrasi, F., 2016. Magma transfer at Campi Flegrei caldera (Italy) before the 1538 AD eruption. Sci. Rep. 6 (1), 32245 https://doi.org/10.1038/srep32245.

Diehl, S. F., Hofstra, A. H., Koenig, A. E., Emsbo, P., Christiansen, W., Johnson, C., 2010. Hydrothermal zebra dolomite in the Great Basin, Nevada—attributes and relation to Paleozoic stratigraphy, tectonics, and ore deposits. Geosphere, 6(5), 663-690.

Doglioni, C., 1991. A proposal for the kinematic modelling of W-dipping subductions-possible applications to the Tyrrhenian-Apennines system: Terra nova, v. 3(4), p. 423-434.

Dong, S., Chen, D., Qing, H., Zhou, X., Wang, D., Guo, Z., Jiang, M., Qian, Y., 2013. Hydrothermal alteration of dolostones in the Lower Ordovician, Tarim Basin, NW China: multiple constraints from petrology, isotope geochemistry and fluid inclusion microthermometry. Marine and Petroleum Geology. 46, 270-286.

Donzé, F., Magnier, S. A., 1995. Formulation of a 3-D numerical model of brittle behaviour. Geophysical Journal International, 122(3), 790-802.

Dreyer, W., 1972. The science of rock mechanics, part 1: the strength properties of rocks (Vol. 1, No. 2).

Druguet, E., Alsop, G. I., Carreras, J., 2009. Coeval brittle and ductile structures associated with extreme deformation partitioning in a multilayer sequence: Journal of Structural Geology, v. 31(5), p. 498-511.

Duan, B., Oglesby, D. D., 2005. The dynamics of thrust and normal faults over multiple earthquake cycles: Effects of dipping fault geometry. Bulletin of the Seismological Society of America, 95(5), 1623-1636.

Duan, Q., Yang, X., Ma, S., Chen, J., Chen, J., 2016. Fluid–rock interactions in seismic faults: Implications from the structures and mineralogical and geochemical compositions of drilling cores from the rupture of the 2008 Wenchuan earthquake, China. Tectonophysics, 666, 260-280.

Duggan, J. P., Mountjoy, E. W., Stasiuk, L. D., 2001. Fault-controlled dolomitization at Swan Hills Simonette oil field (Devonian), deep basin west-central Alberta, Canada. Sedimentology, 48(2), 301-323.

Dunn, D. E., LaFountain, L. J., Jackson, R. E., 1973. Porosity dependence and mechanism of brittle fracture in sandstones. Journal of Geophysical Research, 78(14), 2403-2417.

Eberhardt, E., Stimpson, B., Stead, D., 1999, Effects of grain size on the initiation and propagation thresholds of stress-induced brittle fractures. Rock mechanics and rock engineering, 32, 81-99.

Eichhubl, P., Davatz, N. C., Becker, S. P., 2009. Structural and diagenetic control of fluid migration and cementation along the Moab fault, Utah: AAPG bulletin, v. 93(5), p. 653-681.

Erickson, S. G., 1996. Influence of mechanical stratigraphy on folding vs faulting: Journal of Structural Geology, 18(4), 443-450.

Evans, M. A., Fischer, M. P., 2012. On the distribution of fluids in folds: A review of controlling factors and processes. Journal of Structural Geology, 44, 2-24.

Faccenna, C., Becker, T. W., Lucente, F. P., Jolivet, L., Rossetti, F., 2001. History of subduction and back arc extension in the Central Mediterranean: Geophysical Journal International, v. 145(3), p. 809-820.

Fahy, M. P., Guccione, M. J., 1979. Estimating strength of sandstone using petrographic thin-section data. Bulletin of the Association of Engineering Geologists, 16(4), 467-485.

Fairley, J. P., 2009. Modeling fluid flow in a heterogeneous, fault-controlled hydrothermal system. Geofluids, 9(2), 153-166.

Faulkner, D. R., Jackson, C. A. L., Lunn, R. J., Schlische, R. W., Shipton, Z. K., Wibberley, C. A. J., Withjack, M. O., 2010. A review of recent developments concerning the structure, mechanics and fluid flow properties of fault zones: Journal of Structural Geology, v. 32(11), p. 1557-1575.

Ferranti, L., Oldow, J. S., Sacchi, M., 1996. Pre-Quaternary orogen-parallel extension in the Southern Apennine belt, Italy: Tectonophysics, 260(4), 325-347.

Ferraro, F., Grieco, D. S., Agosta, F., Prosser, G., 2018. Space-time evolution of cataclasis in carbonate fault zones: Journal of Structural Geology, v. 110, p. 45-64.

Ferraro, F., Agosta, F., Prasad, M., Vinciguerra, S., Violay, M., Giorgioni, M., 2020. Pore space properties in carbonate fault rocks of peninsular Italy: Journal of structural geology, 130, 103913.

Ferrill, D. A., Morris, A. P., 2003. Dilational normal faults: Journal of structural geology, v. 25(2), p. 183-196.

Ferrill, D. A., Morris, A. P., 2008. Fault zone deformation controlled by carbonate mechanical stratigraphy, Balcones fault system, Texas: AAPG bulletin, v. 92(3), p. 359-380.

Ferrill, D. A., Morris, A. P., Smart, K. J., 2007. Stratigraphic control on extensional fault propagation folding: Big Brushy Canyon monocline, Sierra del Carmen, Texas: Geological Society, London, Special Publications, v. 292(1), p. 203-217.

Ferrill, D. A., McGinnis, R. N., Morris, A. P., Smart, K. J., Sickmann, Z. T., Bentz, M., Lehrmann, D., Evans, M. A., 2014. Control of mechanical stratigraphy on bed-restricted jointing and normal faulting: Eagle Ford Formation, south-central Texas. AAPG Bulletin, 98(11), 2477-2506.

Ferrill, D. A., Morris, A. P., Wigginton, S. S., Smart, K. J., McGinnis, R. N., Lehrmann, D., 2016. Deciphering thrust fault nucleation and propagation and the importance of footwall synclines: Journal of Structural Geology, v. 85, p. 1-11.

Ferrill, D. A., Morris, A. P., McGinnis, R. N., Smart, K. J., Wigginton, S. S., Hill, N. J., 2017. Mechanical stratigraphy and normal faulting: Journal of Structural Geology, v. 94, p. 275-302.

Ferrill, D. A., Smart, K. J., Cawood, A. J., Morris, A. P., 2021. The fold-thrust belt stress cycle: Superposition of normal, strike-slip, and thrust faulting deformation regimes: Journal of Structural Geology, v. 148, p. 104362.

Fredman, N., Tveranger, J., Semshaug, S., Braathen, A., Sverdrup, E., 2007. Sensitivity of fluid flow to fault core architecture and petrophysical properties of fault rocks in siliciclastic reservoirs: a synthetic fault model study: Petroleum Geoscience, 13(4), 305-320.

Fredrich, J. T., Evans, B., Wong, T. F., 1990. Effect of grain size on brittle and semibrittle strength: Implications for micromechanical modelling of failure in compression. Journal of Geophysical Research: Solid Earth, 95(B7), 10907-10920.

Frehner, M., Schmid, T., 2016. Parasitic folds with wrong vergence: How pre-existing geometrical asymmetries can be inherited during multilayer buckle folding: Journal of Structural Geology, v. 87, p. 19-29.

Gallagher Jr, J. J., Friedman, M., Handin, J., Sowers, G. M., 1974. Experimental studies relating to microfracture in sandstone: Tectonophysics, v. 21(3), p. 203-247.

Galli, A., Grassi, D., Sartori, G., Gianola, O., Burg, J. P., Schmidt, M. W., 2019. Jurassic carbonatite and alkaline magmatism in the Ivrea zone (European Alps) related to the breakup of Pangea. Geology, 47(3), 199-202.

Gao, F., Stead, D., Elmo, D., 2016. Numerical simulation of microstructure of brittle rock using a grain-breakable distinct element grain-based model. Computers and Geotechnics, 78, 203-217.

Gao, J., Zheng, H., Liu, B., Pan, L., Li, R., Wu, J., Yang, X., Tang, H., Dong, Y., 2023. Genetic Mechanism of Structurally Controlled Dolomites Derived from Seawater-Hydrothermal Mixed Fluids—A Case Study from Middle Permian, Central Sichuan Basin, South China. Minerals, 13(6), 758.

Geyer, A., Martí, J., 2014. A short review of our current understanding of the development of ring faults during collapse caldera formation. Front. Earth Sci. 2 https://doi.org/10.3389/feart.2014.00022.

Ghasemi, S., Khamechian, M., Nikudel, M. R., Zalooli, A., 2021. The effect of mineralogy and grain size on stress damage thresholds of granite and diorite. Scientific Quarterly Journal of Iranian Association of Engineering Geology, 13(4), 29-41.

Ghisetti, F., Vezzani, L., 2002. Normal faulting, transcrustal permeability and seismogenesis in the Apennines (Italy). Tectonophysics, 348(1-3), 155-168.

Giaccio, B., Isaia, R., Fedele, F.G., Di Canzio, E., Hoffecker, J., Ronchitelli, A., Sinitsyn, A. A., Anikovich, M., Lisitsyn, S.N., Popov, V.V., 2008. The campanian ignimbrite and codola tephra layers: two temporal/stratigraphic markers for the early upper palaeolithic in southern Italy and eastern Europe. J. Volcanol. Geoth. Res. 177 (1), 208–226. https://doi.org/10.1016/j.jvolgeores.2007.10.007.

Giorgioni, M., Iannace, A., D'Amore, M., Dati, F., Galluccio, L., Guerriero, V., Mazzoli, S., Parente, M., Strauss, C., Vitale, S., 2016. Impact of early dolomitization on multi-scale petrophysical heterogeneities and fracture intensity of low-porosity platform carbonates (Albian-Cenomanian, southern Apennines, Italy): Marine and Petroleum Geology, 73, 462-478. https://doi.org/ 10.1016/j.marpetgeo.2016.03.011

Giorno, M., Barale, L., Bertok, C., Frenzel, M., Looser, N., Guillong, M., Bernasconi, S. M., Martire, L., 2022. Sulfide-associated hydrothermal dolomite and calcite reveal a shallow burial depth for Alpine-type Zn-(Pb) deposits. Geology, 50(7), 853-858.

Gómez-Vasconcelos, M. G., Macías, J. L., Avellán, D. R., Sosa-Ceballos, G., Garduño-Monroy, V. H., Cisneros-Máximo, G., Layer, P., W., Benowitz, J., Lopez-Loera, H., Lopez, F., M., Perton, M., 2020. The control of preexisting faults on the distribution, morphology, and volume of monogenetic volcanism in the Michoacán-Guanajuato Volcanic Field. Bulletin, 132(11-12), 2455-2474.

Grauls, D., Pascaud, F., Rives, T., 2002. Quantitative fault seal assessment in hydrocarbon-compartmentalised structures using fluid pressure data. In Norwegian Petroleum Society Special Publications (Vol. 11, pp. 141-156). Elsevier.

Gregg, J. M., Bish, D. L., Kaczmarek, S. E., Machel, H. G., 2015. Mineralogy, nucleation and growth of dolomite in the laboratory and sedimentary environment: a review. Sedimentology, 62(6), 1749-1769.

Griffith, A. A., 1921. VI. The phenomena of rupture and flow in solids. Philosophical transactions of the royal society of london. Series A, containing papers of a mathematical or physical character, 221(582-593), 163-198.

Grossi, M., Morganti, E., Cassetti, M., 1934. Carta Geologica d'Italia, foglio 16, Isernia. Servizio Geologico d'Italia, scala 1:100,000.

Gudmundsson, A., 1988. Formation of collapse calderas. Geology 16 (9), 808–810. https://doi.org/10.1130/0091-7613(1988)016<0808:FOCC>2.3.CO;2.

Gudmundsson, A., 2000. Active fault zones and groundwater flow. Geophysical Research Letters, 27(18), 2993-2996.

Gudmundsson, A., 2008. Chapter - 8 magma-chamber geometry, fluid transport, local stresses and rock behaviour during collapse caldera formation. In: Gottsmann, J., Martí, J. (Eds.), Developments in Volcanology. Elsevier., Amsterdam, pp. 313–349. https://doi.org/10.1016/S1871-644X(07)000083.

Gudmundsson, A., 2020. Volcanotectonics: Understanding the Structure, Deformation and Dynamics of Volcanoes. Cambridge University Press. https://doi.org/10.1017/9781139176217.

Guerriero, V., Mazzoli, S., Iannace, A., Vitale, S., Carravetta, A., Strauss, C., 2013. A permeability model for naturally fractured carbonate reservoirs: Marine and Petroleum Geology, 40, 115-134. https://doi.org/10.1016/j.marpetgeo.2012.11.002

Guerriero, V., Dati, F., Giorgioni, M., Iannace, A., Mazzoli, S., Vitale, S., 2015. The role of stratabound fractures for fluid migration pathways in well-bedded carbonates: Italian Journal of Geosciences. v. 134, p. 383-395.. https://doi.org/10.3301/IJG.2014.27

Gupta, A. S., Rao, K. S., 2000. Weathering effects on the strength and deformational behaviour of crystalline rocks under uniaxial compression state. Engineering geology, 56(3-4), 257-274.

Haas, J., Budai, T., Hips, K., Czuppon, G., Győri, O., Horváth, A., Héja, G., 2022. Dolomitization of Late Norian carbonate deposits of restricted basin facies in the Keszthely Mts. Transdanubian Range, Hungary. International Journal of Earth Sciences, 111, 245-268.

Hampton, R. L., Bindeman, I. N., Stern, R. A., Coble, M. A., Rooyakkers, S. M., 2021. A microanalytical oxygen isotopic and U-Th geochronologic investigation and modeling of rhyolite petrogenesis at the Krafla Central Volcano, Iceland. Journal of Volcanology and Geothermal Research, 414, 107229.

Han, R., Shimamoto, T., Hirose, T., Ree, J. H., Ando, J. I., 2007. Ultralow friction of carbonate faults caused by thermal decomposition. Science, 316(5826), 878-881.

Hardy, S., Finch, E., 2007. Mechanical stratigraphy and the transition from trishear to kink-band fault-propagation fold forms above blind basement thrust faults: a discrete-element study: Marine and Petroleum Geology, v. 24(2), p. 75-90.

Harris, C., Ashwal, L. D., 2002. The origin of low δ 18 O granites and related rocks from the Seychelles. Contributions to Mineralogy and Petrology, 143, 366-376.

Heap, M.J., Gravley, D.M., Kennedy, B.M., Gilg, H.A., Bertolett, E., Barker, S.L.L., 2020. Quantifying the role of hydrothermal alteration in creating geothermal and epithermal mineral resources: the Ohakuri ignimbrite (Taupo Volcanic Zone, New Zealand). J. Volcanol. Geoth. Res. 390, 106703 https://doi.org/10.1016/j.jvolgeores.2019.106703.

Herrero, M. J., Marfil, R., Escavy, J. I., Scherer, M., Arroyo, X., Martín-Crespo, T., López de Andrés, S., 2020. Hydrothermal activity within a sedimentary succession: aragonites as indicators of Mesozoic Rifting (Iberian Basin, Spain). International Geology Review, 62(1), 94-112.

Hoek, E., Bray, J. D., 1981. Rock slope engineering: CRC press.

Hoek, E., Brown, E.T., 1997. Practical estimates of rock mass strength. Int. J. Rock Mech. Min. Sci. Geomech. Abstr. 34(8): 1165–1186.

Holohan, E.P., Schöpfer, M.P.J., Walsh, J.J., 2011. Mechanical and geometric controls on the structural evolution of pit crater and caldera subsidence. J. Geophys. Res. Solid Earth 116 (B7). https://doi.org/10.1029/2010JB008032.

Hooker, J. N., Laubach, S. E., Marrett, R., 2013. Fracture-aperture size—Frequency, spatial distribution, and growth processes in strata-bounded and non-strata-bounded fractures, Cambrian

Mesón Group, NW Argentina: Journal of Structural Geology, v. 54, p. 54-71.

Hoshino K., 1974. Effect of porosity on the strength of the clastic sedimentary rocks. Proceedings of the 3rd International Congress on Rock Mechanics, Denver, USA, September 1–7, vol. II, Part A, 1974. p. 511–16.

Hu, X., Xie, N., Zhu, Q., Chen, L., Li, P., 2020. Modeling damage evolution in heterogeneous granite using digital image-based grain-based model. Rock Mechanics and Rock Engineering, 1-21.

Huggins, P., Watterson, J., Walsh, J.J., Childs, C., 1995. Relay zone geometry and displacement transfer between normal faults recorded in coal-mine plans. J. Struct. Geol. 17 (12), 1741–1755. https://doi.org/10.1016/0191-8141(95)00071-K.

Hugman Iii, R. H. H., Friedman, M., 1979. Effects of texture and composition on mechanical behavior of experimentally deformed carbonate rocks. AAPG Bulletin, 63(9), 1478-1489.

Iannace, A., Bonardi, G., D'Errico, M., Mazzoli, S., Perrone, V., Vitale, S., 2005b. Structural setting and tectonic evolution of the Apennine Units of northern Calabria. Comptes Rendus Geoscience, 337(16), 1541-1550.

Iannace, A., Capuano, M., Galluccio, L., 2011. “Dolomites and dolomites” in Mesozoic platform carbonates of the Southern Apennines: Geometric distribution, petrography and geochemistry. Palaeogeography, Palaeoclimatology, Palaeoecology. 310(3-4), 324-339.

Iannace, A., Parente, M., Zamparelli, V., 2005a. An early Jurassic submarine scarp in the Western Matese Mountains. Bollettino della Società geologica italiana. 124, 215-221.

Iannace, A., Parente, M., Zamparelli, V., 2005b. The Upper Triassic platform margin facies of Southern Apennines and their Jurassic fate: state of the art. Boll Soc Geol It, 124, 203-214.

Iannace, A., Vitale, S., D'errico, M., Mazzoli, S., Di Staso, Macaione, A., Messina, E., Reddy, S. M., Somma, R., Zamparelli, V., Zattin, M., Bonardi, G., 2007. The carbonate tectonic units of northern Calabria (Italy): a record of Apulian palaeomargin evolution and Miocene convergence, continental crust subduction, and exhumation of HP–LT rocks. Journal of the Geological Society, 164(6), 1165-1186.

Intrieri, E., Di Traglia, F., Del Ventisette, C., Gigli, G., Mugnai, F., Luzi, G., Casagli, N., 2013. Flank instability of Stromboli volcano (Aeolian Islands, Southern Italy): integration of GB-InSAR and geomorphological observations. Geomorphology 201, 60–69.

https://doi.org/10.1016/j.geomorph.2013.06.007.

Isaia, R., D'Antonio, M., Dell'Erba, F., Di Vito, M., Orsi, G., 2004. The Astroni volcano: the only example of closely spaced eruptions in the same vent area during the recent history of the Campi Flegrei caldera (Italy). J. Volcanol. Geoth. Res. 133 (1), 171–192. https://doi.org/10.1016/S0377-0273(03)00397-4.

Isaia, R., Giuseppe, M., Natale, J., Tramparulo, F., Troiano, A., Vitale, S., 2021. Volcano-tectonic setting of the pisciarelli fumarole field, Campi Flegrei caldera, southern Italy: insights into fluid circulation patterns and hazard scenarios. Tectonics. https://doi.org/10.1029/2020TC006227.

Isaia, R., Vitale, S., Di Giuseppe, M.G., Iannuzzi, E., D'Assisi Tramparulo, F., Troiano, A., 2015. Stratigraphy, structure, and volcano-tectonic evolution of Solfatara maar-diatreme (Campi Flegrei, Italy). GSA Bulletin 127 (9–10), 1485–1504. https://doi.org/10.1130/B31183.1.

ISRM 1979 Suggest Methods for Determining Water Content, Porosity, Density, Absorption and Related Properties and Swelling and Slake-Durability Index Properties Int. J. Rock Mech. Min. Sci. Geomech. Abstr. 16 143 – 156

Jackson, J., McKenzie, D., 1983. The geometrical evolution of normal fault systems. Journal of Structural Geology, 5(5), 471-482.

Jackson, C.A.L., Rotevatn, A., 2013. 3D seismic analysis of the structure and evolution of a salt-influenced normal fault zone: a test of competing fault growth models. J. Struct. Geol. 54, 215–234. https://doi.org/10.1016/j.jsg.2013.06.012.

Jackson, C. A. L., Lewis, M. M., 2016. Structural style and evolution of a salt-influenced rift basin margin; the impact of variations in salt composition and the role of polyphase extension: Basin Research, v. 28(1), p. 81-102.

James, M. R., Robson, S., 2012. Straightforward reconstruction of 3D surfaces and topography with a camera: Accuracy and geoscience application: Journal of Geophysical Research: Earth Surface, v. 117(F3).

Jeanne, P., Guglielmi, Y., Lamarche, J., Cappa, F., Marié, L., 2012. Architectural characteristics and petrophysical properties evolution of a strike-slip fault zone in a fractured porous carbonate reservoir: Journal of Structural Geology, v. 44, p. 93-109.

Jébrak, M., 1997. Hydrothermal breccias in vein-type ore deposits: a review of mechanisms, morphology and size distribution: Ore geology reviews, 12(3), 111-134.

Jiang, Y., Zhu, Z., Yu, L., Zhou, L., Zhang, R., Ma, L., 2022. Investigation of the fracture characteristics of granite and green sandstone under different thermal treatments. Theoretical and Applied Fracture Mechanics, 118, 103217.

Jinari, A., Rddad, L., Mouguina, E. M., Ouadjou, A., 2023. Origin of the Amensif Zn-Cu (Pb-Ag-Au) distal skarn deposit (Western High Atlas, Morocco): Constraints from COS isotopes. Journal of African Earth Sciences, 199, 104850.

Jolie, E., Scott, S., Faulds, J., Chambefort, I., Axelsson, G., Gutiérrez-Negrín, L. C., Regenspurg, S., Ziegler, M., Ayling, B., Richter, A., Zemedkun, M. T., 2021. Geological controls on geothermal resources for power generation. Nature Reviews Earth & Environment, 2(5), 324-339.

Ju M, Xing H., 2022. Crack propagation in jointed rock and its effect on rock macrofracture resistance: insights from discrete element analysis. Geomechanics and Geophysics for Geo-Energy and Geo-Resources, 8, 1–22.

Ju, M., Li, X., Li, X., Zhang, G., 2022. A review of the effects of weak interfaces on crack propagation in rock: From phenomenon to mechanism. Engineering Fracture Mechanics, 263, 108297.

Juez-Larré, J., Ter Voorde, M., 2009. Thermal impact of the break-up of Pangea on the Iberian Peninsula, assessed by thermochronological dating and numerical modelling. Tectonophysics, 474(1-2), 200-213.

Kaminskaite, I., Fisher, Q. J., Michie, E. A. H., 2019. Microstructure and petrophysical properties of deformation bands in high porosity carbonates: Journal of Structural Geology, v. 119, p. 61-80.

Kataoka, M., Obara, Y., Kuruppu, M., 2015. Estimation of fracture toughness of anisotropic rocks by semi-circular bend (SCB) tests under water vapor pressure. Rock Mechanics and Rock Engineering, 48, 1353-1367.

Kaus, B. J., 2010. Factors that control the angle of shear bands in geodynamic numerical models of brittle deformation. Tectonophysics, 484(1-4), 36-47.

Kelsall, P., C., Watters, R., J., Franzone J., G., 1986. Engineering characterization of fissured, weathered dolerite and vesicular basalt. Proceedings of the 27th US Symposium on Rock Mechanics: Key to Energy Production, Tuscaloosa, USA, June 23–25, , p. 77–84.

Kennedy, B., Stix, J., Vallance, J.W., Lavallée, Y., Longpré, M.A., 2004. Controls on caldera structure: results from analogue sandbox modeling. GSA Bulletin 116 (5–6), 515–524. https://doi.org/10.1130/B25228.1.

Kim, Y.S., Peacock, D.C., Sanderson, D.J., 2004. Fault damage zones. J. Struct. Geol. 26 (3), 503–517. https://doi.org/10.1016/j.jsg.2003.08.002.

Kirby, E., Whipple, K. X., 2012. Expression of active tectonics in erosional landscapes. Journal of structural geology, 44, 54-75.

Knipe, R. J., Jones, G., Fisher, Q. J., 1998. Faulting, fault sealing and fluid flow in hydrocarbon reservoirs: an introduction. Geological Society, London, Special Publications, 147(1), vii-xxi.

Kranz, R. L., 1979. Crack-crack and crack-pore interactions in stressed granite. Int. J. Rock Mech. Min. Sci. Geomech. Abstr. 16 (1), 37-47.

Kristensen, M.B., Childs, C.J., Korstgård, J.A., 2008. The 3D geometry of small-scale relay zones between normal faults in soft sediments. J. Struct. Geol. 30 (2), 257–272. https://doi.org/10.1016/j.jsg.2007.11.003.

Kwasniewski, M. A., 1993. Mechanical behavior of anisotropic rocks. Comprehensive rock engineering, 1, 285-312.

Kylander-Clark, A. R., 2020. Expanding the limits of laser-ablation U–Pb calcite geochronology. Geochronology, 2(2), 343-354.

Lamarche, J., Lavenu, A. P., Gauthier, B. D., Guglielmi, Y., Jayet, O., 2012. Relationships between fracture patterns, geodynamics and mechanical stratigraphy in Carbonates (South-East Basin, France). Tectonophysics, 581, 231-245.

Lan, H., Martin, C. D., Hu, B., 2010. Effect of heterogeneity of brittle rock on micromechanical extensile behavior during compression loading. Journal of Geophysical Research: Solid Earth, 115(B1).

Lan, Z., Wu, S., Wang, F., Liu, B., Shi, K., Sun, J., Cao, R., Li, X. H., 2023. A ca. 290 Ma hydrothermal calcite in Cambrian dolostone. Marine and Petroleum Geology. 147, 106011.

Langone, A., Zanetti, A., Daczko, N. R., Piazolo, S., Tiepolo, M., Mazzucchelli, M., 2018. Zircon U-Pb dating of a lower crustal shear zone: A case study from the northern sector of the Ivrea-Verbano

Zone (Val Cannobina, Italy). Tectonics, 37(1), 322-342.

Lapponi, F., Bechstaedt, T., Boni, M., Banks, D. A., Schneider, J., 2014. Hydrothermal dolomitization in a complex geodynamic setting (Lower Palaeozoic, northern Spain). Sedimentology, 61(2), 411-443.

Larsen B, Gudmundsson A, Grunnaleite I, Sælen G, Talbot MR, Buckley SJ., 2010. Effects of sedimentary interfaces on fracture pattern, linkage, and cluster formation in peritidal carbonate rocks. Mar Pet Geol, 27,1531–50.

Laubach, S. E., Olson, J. E., Gross, M. R., 2009. Mechanical and fracture stratigraphy: AAPG bulletin, v. 93(11), p. 1413-1426.

Laubach, S. E., Lamarche, J., Gauthier, B. D., Dunne, W. M., Sanderson, D. J., 2018. Spatial arrangement of faults and opening-mode fractures: Journal of Structural Geology, v. 108, p. 2-15.

Lavoie, D., Chi, G., Urbatsch, M., Davis, W. J., 2010. Massive dolomitization of a pinnacle reef in the Lower Devonian West Point Formation (Gaspé Peninsula, Quebec): An extreme case of hydrothermal dolomitization through fault-focused circulation of magmatic fluids. AAPG bulletin, 94(4), 513-531.

Li, X. F., Li, H. B., Liu, L. W., Liu, Y. Q., Ju, M. H., Zhao, J., 2020. Investigating the crack initiation and propagation mechanism in brittle rocks using grain-based finite-discrete element method. International Journal of Rock Mechanics and Mining Sciences, 127, 104219.

Li, X. F., Li, H. B., Zhao, J., 2021. Transgranular fracturing of crystalline rocks and its influence on rock strengths: Insights from a grain-scale continuum–discontinuum approach. Computer Methods in Applied Mechanics and Engineering, 373, 113462.

Liang, C., Cao, Y., Liu, K., Jiang, Z., Wu, J., Hao, F., 2018. Diagenetic variation at the lamina scale in lacustrine organic-rich shales: Implications for hydrocarbon migration and accumulation. Geochimica et Cosmochimica Acta, 229, 112-128.

Liu, Y., Jiao, X., Li, H., Yuan, M., Yang, W., Zhou, X., Zheng, C., Sun, Q., Wang, S., 2012. Primary dolostone formation related to mantle-originated exhalative hydrothermal activities, Permian Yuejingou section, Santanghu area, Xinjiang, NW China. Science China Earth Sciences. 55, 183-192.

Lockner, D. A., Beeler, N. M., 2002. Rock failure and earthquakes. International Geophysics

Series, 81(A), 505-538.

Lorenz, V., 1975. Formation of phreatomagmatic maar–diatreme volcanoes and its relevance to kimberlite diatremes. In: Ahrens, L.H., Dawson, J.B., Duncan, A.R., Erlank, A.J. (Eds.), Physics and Chemistry of the Earth. Pergamon, Oxford, pp. 17–27. https://doi.org/10.1016/B978-0-08-018017-5.50006-7.

Lorenz, V., 1986. On the growth of maars and diatremes and its relevance to the formation of tuff rings. Bull. Volcanol. 48 (5), 265–274. https://doi.org/10.1007/BF01081755.

Lorenz, V., Kurszlaukis, S., 2007. Root zone processes in the phreatomagmatic pipe emplacement model and consequences for the evolution of maar–diatreme volcanoes. J. Volcanol. Geoth. Res. 159 (1), 4–32. https://doi.org/10.1016/j.jvolgeores.2006.06.019.

Lugli, S., Morteani, G., Blamart, D., 2002. Petrographic, REE, fluid inclusion and stable isotope study of magnesite from the Upper Triassic Burano Evaporites (Secchia Valley, northern Apennines): contributions from sedimentary, hydrothermal and metasomatic sources. Mineralium Deposita, 37, 480–494. https://doi.org/10.1007/s00126-001-0251-6

Lustrino, M., Abbas, H., Agostini, S., Caggiati, M., Carminati, E., Gianolla, P., 2019. Origin of Triassic magmatism of the Southern Alps (Italy): constraints from geochemistry and Sr-Nd-Pb isotopic ratios. Gondwana Research, 75, 218-238.

Lyu, W., Zeng, L., Lyu, P., Yi, T., Dong, S., Wang, S., Xu, X., Chen, H., 2022. Insights into the mechanical stratigraphy and vertical fracture patterns in tight oil sandstones: The Upper Triassic Yanchang Formation in the eastern Ordos Basin, China: Journal of Petroleum Science and Engineering, v. 212, p. 110247.

Macedonio, G., Giudicepietro, F., D'auria, L., Martini, M., 2014. Sill intrusion as a source mechanism of unrest at volcanic calderas. J. Geophys. Res. Solid Earth 119 (5), 3986–4000. https://doi.org/10.1002/2013JB010868.

Machel, H. G., 2004. Concepts and models of dolomitization: a critical reappraisal. Geological Society, London, Special Publications, 235(1), 7-63.

Magee, C., Bastow, I.D., van Wyk de Vries, B., Jackson, C.A.L., Hetherington, R., Hagos, M., Hoggett, M., 2017. Structure and dynamics of surface uplift induced by incremental sill emplacement. Geology 45 (5), 431–434. https://doi.org/10.1130/G38839.1.

Manzocchi, T., Childs, C., Walsh, J. J., 2010. Faults and fault properties in hydrocarbon flow models. Geofluids, 10(1-2), 94-113.

Marchal, D., Guiraud, M., Rives, T., 2003. Geometric and morphologic evolution of normal fault planes and traces from 2D to 4D data. J. Struct. Geol. 25 (1), 135–158. https://doi.org/10.1016/S0191-8141(02)00011-1.

Martel, S. J., 1999, Mechanical controls on fault geometry. Journal of Structural Geology, 21(6), 585-596.

Marti, J., Felpeto, A., 2010. Methodology for the computation of volcanic susceptibility: an example for mafic and felsic eruptions on Tenerife (Canary Islands). Journal of Volcanology and Geothermal Research, 195(1), 69-77.

Marturano, A., Isaia, R., Aiello, G., Barra, D., 2018. Complex dome growth at Campi Flegrei caldera (Italy) in the last 15 ka. J. Geophys. Res. Solid Earth 123 (9), 8180–8197. https://doi.org/10.1029/2018JB015672.

Mathieu, L., De Vries, B. V. W., Holohan, E. P., Troll, V. R., 2008. Dykes, cups, saucers and sills: Analogue experiments on magma intrusion into brittle rocks. Earth and Planetary Science Letters, 271(1-4), 1-13.

Mazzoli, S., D'errico, M., Aldega, L., Corrado, S., Invernizzi, C., Shiner, P., Zattin, M., 2008. Tectonic burial and "young"(< 10 Ma) exhumation in the southern Apennines fold-and-thrust belt (Italy): Geology, v. 36(3), p. 243-246.

McArthur J.M., Howarth R.J., Shields G.A. Zhou Y., 2020. Strontium isotope stratigraphy, Chapter 7, p211 - p238 In: Gradstein F.M., Ogg J.G., Schmitz M.D., Ogg G.M., (Eds), A Geologic Time Scale, Elsevier. 2(1), 1357-2020.

McCalpin, J. P., 2009. Application of paleoseismic data to seismic hazard assessment and neotectonic research. International Geophysics, 95, 1-106.

McGrath, A.G., Davison, I., 1995. Damage zone geometries around fault tips: Journal Structural Geology, 17, 1011–1024.

McGuire, W.J., 2006. Lateral collapse and tsunamigenic potential of marine volcanoes. Geol. Soc.London.Special Publ 269 (1), 121–140. https://doi.org/10.1144/GSL.SP.2006.269.01.08.

Menéndez, B., Zhu, W., Wong, T. F., 1996. Micromechanics of brittle faulting and cataclastic flow in Berea sandstone. Journal of structural geology, 18(1), 1-16.

Micarelli, L., Benedicto, A., Wibberley, C. A. J., 2006. Structural evolution and permeability of normal fault zones in highly porous carbonate rocks. Journal of Structural Geology, 28(7), 1214-1227.

Michie, E. A. H., Haines, T. J., 2016. Variability and heterogeneity of the petrophysical properties of extensional carbonate fault rocks, Malta: Petroleum Geoscience, 22(2), 136-152.

Mooney, W. D., Ginzburg, A., 1986. Seismic measurements of the internal properties of fault zones. Pure and Applied Geophysics, 124, 141-157.

Morris, A. P., Ferrill, D. A., McGinnis, R. N., 2009. Mechanical stratigraphy and faulting in Cretaceous carbonates: AAPG bulletin, v. 93(11), p. 1459-1470.

Morrow, C. A., Lockner, D. A., 2001. Hayward fault rocks: Porosity, density and strength measurements. US Department of the Interior, US Geological Survey.

Mosher, S., Berger, R. L., Anderson, D. E., 1975. Fracturing characteristics of two granites. Rock Mech. 7 (3), 167-176.

Mostardini, F., Merlini, S., 1986. Appennino centro-meridionale: Sesioni geologiche e proposta di modello strutturale. In: Geologia dell'Italia centrale. Congresso nazionale. 73, 147-149.

Mountjoy, E. W., Qing, H., McNutt, R. H., 1992. Strontium isotopic composition of Devonian dolomites, Western Canada Sedimentary Basin: significance of sources of dolomitizing fluids. Applied Geochemistry, 7(1), 59-75.

Mozafari, M., Swennen, R., Balsamo, F., El Desouky, H., Storti, F., Taberner, C., 2019. Fault-controlled dolomitization in the Montagna dei Fiori Anticline (Central Apennines, Italy): record of a dominantly pre-orogenic fluid migration. Solid Earth. 10(4), 1355-1383.

Nasseri, M. H. B., Mohanty, B., Robin, P. Y., 2005. Characterization of microstructures and fracture toughness in five granitic rocks. International journal of rock mechanics and mining sciences, 42(3), 450-460.

Nasseri, M. H. B., Grasselli, G., Mohanty, B., 2010. Fracture toughness and fracture roughness in anisotropic granitic rocks. Rock Mechanics and Rock Engineering, 43, 403-415.

Natale, J., Ferranti, L., Marino, C., Sacchi, M., 2020. Resurgent dome faults in the offshore of the Campi Flegrei caldera (Pozzuoli Bay, Campania): preliminary results from high-resolution seismic reflection profiles. Boll. Geofis. Teor. Appl. 61 (3) https://doi.org/10.4430/bgta0315.

Natale, J., Ferranti, L., Isaia, R., Marino, C., Sacchi, M., Spiess, V., Vitale, S., 2022. Integrated on-land-offshore stratigraphy of the Campi Flegrei caldera: new insights into the volcano-tectonic evolution in the last 15 kyr. Basin Res. https://doi.org/10.1111/bre.12643.

Nayebi, N., Esmaeily, D., D'Antonio, M., Xia, X., Renzo, V. D., Lehmann, B., Shinjo, R., Babazadeh, S., Deevsalar, R., Modabberi, S., 2023. Zircon U–Pb ages and Sr–Nd–Pb–Hf isotopic compositions constrain the tectono-magmatic evolution of the Anomaly 21-A iron ore region, Bafq metallogenic province, Central Iran. Journal of Asian Earth Sciences. 250, 105646.

Nelson, R. A., 1985. Geologic analysis of naturally fractured reservoirs: Huston, Gulf Professional Publishing.

Nemat-Nasser, S., Horii, H., 1982. Compression-induced nonplanar crack extension with application to splitting, exfoliation, and rockburst. Journal of Geophysical Research: Solid Earth, 87(B8), 6805-6821.

Nicol, A., Robinson, R., Dissen, R.V., Harvison, A., 2016. Variability of recurrence interval and single-event slip for surface-rupturing earthquakes in New Zealand. N. Z. J. Geol. Geophys. 59 (1), 97–116. https://doi.org/10.1080/00288306.2015.1127822.

Nicol, A., Walsh, J., Childs, C., Manzocchi, T., 2020. Chapter 6 - the growth of faults. In: Tanner, D., Brandes, C. (Eds.), Understanding Faults. Elsevier., Amsterdam, pp. 221–255. https://doi.org/10.1016/B978-0-12-815985-9.00006-0.

Nicol, A., Walsh, J.J., Villamor, P., Seebeck, H., Berryman, K.R., 2010. Normal fault interactions, paleoearthquakes and growth in an active rift. J. Struct. Geol. 32 (8), 1101–1113. https://doi.org/10.1016/j.jsg.2010.06.018.

Noguera, A. M., Rea, G., 2000. Deep structure of the Campanian–Lucanian arc (southern Apennine, Italy). Tectonophysics, 324(4), 239-265.

Nuriel, P., Wotzlaw, J. F., Ovtcharova, M., Vaks, A., Stremtan, C., Šala, M., Roberts, N. M. W., Kylander-Clark, A. R. C., 2012. The use of ASH-15 flowstone as a matrix-matched reference material for laser-ablation U-Pb geochronology of calcite, Geochronology, 3, 35-47, 10.5194/gchron-3-35-2021.

Ogata, K., Storti, F., Balsamo, F., Tinterri, R., Bedogni, E., Fetter, M., Gomes, L., Hatushika, R., 2017. Sedimentary facies control on mechanical and fracture stratigraphy in turbidites. Bulletin, 129(1-2), 76-92.

Oliveira, L. S. B., Nogueira, F. C. C., Vasconcelos, D. L., Balsamo, F., Bezerra, F. H. R., Pérez, Y. A. R., 2022. Mechanical stratigraphy influences deformation band pattern in arkosic sandstones, Rio do Peixe Basin, Brazil: Journal of Structural Geology, v. 155, p. 104510.

Olsson, W. A., 1974. Grain size dependence of yield stress in marble. Journal of Geophysical Research, 79(32), 4859-4862.

Orsi, G., Di Vito, M. A., Isaia, R., 2004. Volcanic hazard assessment at the restless Campi Flegrei caldera. Bulletin of Volcanology, 66, 514-530.

Ortega, O. J., Gale, J. F., Marrett, R., 2010. Quantifying diagenetic and stratigraphic controls on fracture intensity in platform carbonates: An example from the Sierra Madre Oriental, northeast Mexico: Journal of Structural Geology, v. 32(12), p. 1943-1959.

Pagel, M., Bonifacie, M., Schneider, D. A., Gautheron, C., Brigaud, B., Calmels, D., Cros, A., Saint-Bezar, B., Landrein, P., Sutcliffe, C., Davis, D., Chaduteau, C., 2018. Improving paleohydrological and diagenetic reconstructions in calcite veins and breccia of a sedimentary basin by combining Δ47 temperature, δ18Owater and U-Pb age, Chem Geol, 481, 1-17, https://doi.org/10.1016/j.chemgeo.2017.12.026.

Paradis, S., Hannigan, P., Dewing, K. 2007. Mississippi Valley-type lead-zinc deposits. Mineral deposits of Canada: A synthesis of major deposit-types, district metallogeny, the evolution of geological provinces, and exploration methods. Geological Association of Canada, Mineral Deposits Division, Special Publication, 5, 185-203.

Passchier, C. W., Trouw, R. A., 2005. Microtectonics. Springer Science & Business Media.

Patacca, E., Scandone, P., 2007. Geology of the southern Apennines: Bollettino della Società Geologica Italiana, v. 7, p. 75-119.

Paterson, M. S., 1958. Experimental deformation and faulting in Wombeyan marble. Geological Society of America Bulletin, 69(4), 465-476.

Paterson, M. S., Wong, T. F., 2005. Experimental rock deformation: the brittle field (Vol. 348). Berlin: Springer.

Peacock, D.C.P., 2002. Propagation, interaction and linkage in normal fault systems. Earth Sci. Rev. 58 (1), 121–142. https://doi.org/10.1016/S0012-8252(01)00085-X.

Peacock, D.C.P., Sanderson, D.J., 1991. Displacements, segment linkage and relay ramps in normal fault zones. J. Struct. Geol. 13 (6), 721–733. https://doi.org/10.1016/0191-8141(91)90033-F.

Peacock, D.C.P., Sanderson, D. J., 1992. Effects of layering and anisotropy on fault geometry: Journal of the Geological Society, 149(5), 793-802.

Peacock, D.C.P., Zhang, X., 1993. Field examples and numerical modelling of oversteps and bends along normal faults in cross-section: Tectonophysics, 234, 147–167.

Peacock, D.C.P., Sanderson, D.J., 1994. Strain and scaling of faults in the chalk at Flamborough Head, U.K. J. Struct. Geol. 16 (1), 97–107. https://doi.org/10.1016/0191-8141(94)90021-3.

Peacock, D. C. P., Mann, A., 2005. Evaluation of the controls on fracturing in reservoir rocks: Journal of Petroleum Geology, 28(4), 385-396.

Peng, J., Xu, C., Dai, B., Sun, L., Feng, J., Huang, Q., 2022. Numerical investigation of brittleness effect on strength and microcracking behavior of crystalline rock. International Journal of Geomechanics, 22(10), 04022178.

Perkins, W. G., 1984. Mount Isa silica dolomite and copper orebodies; the result of a syntectonic hydrothermal alteration system: Economic Geology, 79(4), 601-637.

Person, M., Banerjee, A., Hofstra, A., Sweetkind, D., Gao, Y., 2008. Hydrologic models of modern and fossil geothermal systems in the Great Basin: Genetic implications for epithermal Au-Ag and Carlin-type gold deposits. Geosphere, 4(5), 888-917.

Pfiffner, O. A., 1993. The structure of the Helvetic nappes and its relation to the mechanical stratigraphy: Journal of structural Geology, v. 15(3-5), p. 511-521.

Pizzati, M., Balsamo, F., Storti, F., 2020. Displacement-dependent microstructural and petrophysical properties of deformation bands and gouges in poorly lithified sandstone deformed at shallow burial depth (Crotone Basin, Italy): Journal of Structural Geology, v. 137, p. 104069.

Pollard DD, Aydin A., 1988. Progress in understanding jointing over the past century. Geol Soc Am Bull, 100:1181–204.

Poppe, S., Holohan, E.P., Pauwels, E., Cnudde, V., Kervyn, M., 2015. Sinkholes, pit craters, and small calderas: analog models of depletion-induced collapse analyzed by computed X-ray microtomography GSA. Bulletin 127 (1–2), 281–296. https://doi.org/10.1130/B30989.1,2015.

Přikryl, R., 2001. Some microstructural aspects of strength variation in rocks. International Journal of Rock Mechanics and Mining Sciences, 38(5), 671-682.

Prokoph, A., Shields G.A., Veizer J., 2008. Compilation and time-series analysis of a marine carbonate δ18O, δ13C, 87Sr/86Sr and δ34S database through Earth history. Earth-Science Reviews, 87, 113–133.

Putz-Perrier, M. W., Sanderson, D. J., 2008. Spatial distribution of brittle strain in layered sequences: Journal of Structural Geology, 30(1), 50-64.

Ramamurthy, T., 1993. Strength and modulus responses of anisotropic rocks. Comprehensive rock engineering, 1(13), 313-329.

Ramsay, J. G., Huber, M. I., 1987. Modern structural geology. Folds and Fractures, 2, 309-700.

Rath, A., Exner, U., Tschegg, C., Grasemann, B., Laner, R., Draganits, E., 2011. Diagenetic control of deformation mechanisms in deformation bands in a carbonate grainstone: AAPG bulletin, v. 95(8), p. 1369-1381.

Rawling, G. C., Goodwin, L. B., Wilson, J. L., 2001. Internal architecture, permeability structure, and hydrologic significance of contrasting fault-zone types: Geology, 29(1), 43-46.

Reimer, J. D., Hudema, T., Viau, C., 2001. TSR-HTD ten years later: an exploration update, with examples from western and eastern Canada. The CSPG Annual Convention, 2001

Reiter F., Acs P., 1996. TectonicsFP software: Version 1.6.4, build 1.161 (http://www.tectonicsfp.com).

Rippa, F., Vinale, F., 1983. Structure and mechanical behaviour of a volcanic tuff. In 5th ISRM Congress. OnePetro.

Rizzo, R. E., Inskip, N. F., Fazeli, H., Betlem, P., Bisdom, K., Kampman, N., Snippe, J., Senger, K., Doster, F., Busch, A., 2024. Modelling geological CO2 leakage: Integrating fracture permeability and fault zone outcrop analysis. International Journal of Greenhouse Gas Control, 133, 104105.

Roberts, N. M., Rasbury, E. T., Parrish, R. R., Smith, C. J., Horstwood, M. S., Condon, D. J., 2017. A calcite reference material for LA-ICP-MS U-Pb geochronology. Geochemistry, Geophysics, Geosystems, 18(7), 2807-2814.

Robertson, E. C., 1955. Experimental study of the strength of rocks. Geological Society of America Bulletin, 66(10), 1275-1314.

Robustini, P., Corrado, S., Di Bucci, D., Calabro, R. A., Tornaghi, M., 2003. Comparison between contractional deformation styles in the Matese Mountain: implications for shortening rates in the Apennines. Bollettino Società Geologica Italiana. 122(2), 295-306.

Roche, O., Druitt, T.H., Merle, O., 2000. Experimental study of caldera formation. J. Geophys. Res. Solid Earth 105 (B1), 395–416. https://doi.org/10.1029/1999JB900298.

Roche, V., Camanni, G., Childs, C., Manzocchi, T., Walsh, J., Conneally, J., Saqab, M.M., Delogkos, E., 2021. Variability in the three-dimensional geometry of segmented normal fault surfaces. Earth Sci. Rev. 216, 103523 https://doi.org/10.1016/j.earscirev.2021.103523.

Roche, V., Childs, C., Madritsch, H., Camanni, G., 2020. Layering and structural inheritance controls on fault zone structure in three dimensions: a case study from the northern Molasse Basin, Switzerland. J. Geol. Soc.

Roche, V., Homberg, C., Rocher, M., 2012. Architecture and growth of normal fault zones in multilayer systems: a 3D field analysis in the South-Eastern Basin, France: Journal of Structural Geology, v. 37, p. 19-35.

Ronchi, P., Jadoul, F., Ceriani, A., Di Giulio, A., Scotti, P., Ortenzi, A., Previde Massara, E., 2011. Multistage dolomitization and distribution of dolomitized bodies in Early Jurassic carbonate platforms (Southern Alps, Italy). Sedimentology, 58(2), 532-565.

Ronchi, P., Masetti, D., Tassan, S., Camocino, D. 2012. Hydrothermal dolomitization in platform and basin carbonate successions during thrusting: a hydrocarbon reservoir analogue (Mesozoic of Venetian Southern Alps, Italy). Marine and Petroleum Geology, 29(1), 68-89.

Rowland, J. V., Sibson, R. H., 2004. Structural controls on hydrothermal flow in a segmented rift system, Taupo Volcanic Zone, New Zealand. Geofluids, 4(4), 259-283.

Rykkelid, E., Fossen, H., 2002. Layer rotation around vertical fault overlap zones: observations from seismic data, field examples, and physical experiments: Mar. Pet. Geol. 19, 181–192.

Sabatakakis, N., Koukis, G., Tsiambaos, G., Papanakli, S., 2008. Index properties and strength variation controlled by microstructure for sedimentary rocks. Engineering geology, 97(1-2), 80-90.

Sabbatino, M., Vitale, S., Tavani, S., Consorti, L., Corradetti, A., Cipriani, A., Arienzo, I., Parente, M., 2020. Constraining the onset of flexural subsidence and peripheral bulge extension in the Miocene foreland of the southern Apennines (Italy) by Sr-isotope stratigraphy: Sedimentary geology, v. 401, p. 105634.

Sabbatino, M., Tavani, S., Vitale, S., Ogata, K., Corradetti, A., Consorti, L., Arienzo, I., Cipriani, A., Parente, M., 2021. Forebulge migration in the foreland basin system of the central-southern Apennine fold-thrust belt (Italy): New high-resolution Sr-isotope dating constraints. Basin Research, 33(5), 2817-2836.

Sammis, C. G., Biegel, R. L., 1989. Fractals, fault-gouge, and friction: Pure and Applied Geophysics, v. 131, p. 255-271.

Sammis, C., King, G., Biegel, R., 1987. The kinematics of gouge deformation: Pure and Applied Geophysics, v. 125, p. 777-812.

Sandulli, R., Raspini, A., 2004. Regional to global correlation of lower Cretaceous (Hauterivian–Barremian) shallow-water carbonates of the southern Apennines (Italy) and Dinarides (Montenegro), southern Tethyan Margin. Sedimentary Geology. 165(1-2), 117-153.

Santantonio, M., Carminati, E., 2011. Jurassic rifting evolution of the Apennines and Southern Alps (Italy): Parallels and differences. Bulletin. 123(3-4), 468-484.

Scandone, P., 1967. Studi di geologia lucana: la serie calcareo-silico-marnosa e i suoi rapporti con l'Appennino calcareo. Bollettino Società Naturalisti, Napoli. 76, 1 - 175.

Schaltegger, U., Ulianov, A., Müntener, O., Ovtcharova, M., Peytcheva, I., Vonlanthen, P., Vennemann, T., Antognini, M., Girlanda, F., 2015. Megacrystic zircon with planar fractures in miaskite-type nepheline pegmatites formed at high pressures in the lower crust (Ivrea Zone, southern Alps, Switzerland). American Mineralogist, 100(1), 83-94.

Scholz, C. H., 1987. Wear and gouge formation in brittle faulting: Geology, v. 15(6), p. 493-495.

Scholz, C. H., Gupta, A., 2000. Fault interactions and seismic hazard. Journal of Geodynamics, 29(3-5), 459-467.

Scholz, C. H., Tan, Y. J., Albino, F., 2019. The mechanism of tidal triggering of earthquakes at mid-ocean ridges. Nature communications, 10(1), 2526.

Schöpfer, M. P., Childs, C., Walsh, J. J., 2006. Localisation of normal faults in multilayer sequences: Journal of Structural Geology, v. 28(5), p. 816-833.

Schöpfer, M. P., Childs, C., Walsh, J. J., Manzocchi, T., Koyi, H. A., 2007. Geometrical analysis of the refraction and segmentation of normal faults in periodically layered sequences: Journal of Structural Geology, v. 29(2), p. 318-335.

Schöpfer, M. P., Childs, C., Walsh, J. J., Manzocchi, T., 2016. Evolution of the internal structure of fault zones in three-dimensional numerical models of normal faults. Tectonophysics, 666, 158-163.

Schröckenfuchs, T., Bauer, H., Grasemann, B., Decker, K., 2015. Rock pulverization and localization of a strike-slip fault zone in dolomite rocks (Salzach–Ennstal–Mariazell–Puchberg fault, Austria). Journal of Structural Geology, 78, 67-85.

Schuck, B., Desbois, G., Urai, J. L., 2020. Grain-scale deformation mechanisms and evolution of porosity in experimentally deformed Boom Clay. Journal of Structural Geology, 130, 103894.

Schuck, B., Janssen, C., Schleicher, A. M., Toy, V. G., Dresen, G., 2018. Microstructures imply cataclasis and authigenic mineral formation control geomechanical properties of New Zealand's Alpine Fault. Journal of Structural Geology, 110, 172-186.

Schultz, R. A., 2019. Geologic fracture mechanics: Cambridge University Press. Sequences: Journal of Structural Geoloy, 30, 50–64.

Scibek, J., 2020. Multidisciplinary database of permeability of fault zones and surrounding protolith rocks at world-wide sites. Scientific Data, 7(1), 95.

Shackleton, J. R., Cooke, M. L., Sussman, A. J., 2005. Evidence for temporally changing mechanical stratigraphy and effects on joint-network architecture: Geology, v. 33(2), p. 101-104.

Shah M.M., Nader F.H., Garcia D., Swennen R. Ellam R., 2012. Hydrothermal dolomites in the Early Albian (Cretaceous) platform carbonates (NW Spain): nature and origin of dolomites and dolomitizing fluids. Oil Gas Sci. Technol. 67: 97-122.

Sharp, I., Gillespie, P., Morsalnezhad, D., Taberner, C., Karpuz, R., Vergés, J., Horboury, A., Pickard, N., Garland, J., Hunt, D., 2010. Stratigraphic architecture and fracture-controlled dolomitization of the Cretaceous Khami and Bangestan groups: an outcrop case study, Zagros Mountains, Iran. Geological Society, London, Special Publications. 329(1), 343-396.

Shikazono, N., Hoshino, M., Utada, M., Nakata, M., Ueda, A., 1998. Hydrothermal carbonates in altered wall rocks at the Uwamuki Kuroko deposits, Japan. Mineralium Deposita, 33, 346-358.

Shiner, P., Beccacini, A., Mazzoli, S., 2004. Thin-skinned versus thick-skinned structural models for Apulian carbonate reservoirs: constraints from the Val d'Agri Fields, S Apennines, Italy: Marine and Petroleum Geology, 21(7), 805-827.

Sibley, D. F., Gregg, J. M., 1987. Classification of dolomite rock textures. Journal of sedimentary Research. 57(6), 967-975.

Sibson, R. H., 1977. Fault rocks and fault mechanisms: Journal of the Geological Society, v. 133(3), p. 191-213.

Sibson, R. H., 2000. Fluid involvement in normal faulting. Journal of Geodynamics, 29(3-5), 469-499.

Sibson, R. H., White, S. H., Atkinson, B. K., 1981. Structure and distribution of fault rocks in the Alpine Fault Zone, New Zealand. Geological Society, London, Special Publications, 9(1), 197-210.

Siler, D.L., Faulds, J.E., Mayhew, B., McNamara, D.D., 2016. Analysis of the favorability for geothermal fluid flow in 3D: astor Pass geothermal prospect, Great Basin, northwestern Nevada, USA. Geothermics 60, 1–12. https://doi.org/10.1016/j.geothermics.2015.11.002.

Smeraglia, L., Bettucci, A., Billi, A., Carminati, E., Cavallo, A., Di Toro, G., Natali, M., Passeri, D., Rossi, M., Spagnuolo, E., 2017. Microstructural evidence for seismic and aseismic slips along clay-bearing, carbonate faults. Journal of Geophysical Research: Solid Earth, 122(5), 3895-3915.

Smeraglia, L., Looser, N., Fabbri, O., Choulet, F., Guillong, M., Bernasconi, S. M., 2021. U–Pb dating of middle Eocene–Pliocene multiple tectonic pulses in the Alpine foreland. Solid

Earth, 12(11), 2539-2551.

Smorodinov, M. I., Motovilov, E. A., Volkov, V. A., 1970. Determinations of correlation relationships between strength and some physical characteristics of rocks. In ISRM Congress (pp. ISRM-2CONGRESS). ISRM.

Sorkhabi, R., Tsuji Y., 2005. Faults, Fluid Flow, & Petroleum Traps, Am. Assoc. Petrol. Geol. Mem., 85 (), pp. 1-31

Spangenberg, J., Fontboté, L., Sharp, Z. D., Hunziker, J., 1996. Carbon and oxygen isotope study of hydrothermal carbonates in the zinc-lead deposits of the San Vicente district, central Peru: A quantitative modeling on mixing processes and CO2 degassing. Chemical Geology, 133(1-4), 289-315.

Spencer-Cervato, C., Mullis, J., 1992. Chemical study of tectonically controlled hydrothermal dolomitization: an example from the Lessini Mountains, Italy. Geologische Rundschau. 81, 347-370.

Sperrevik, S., Gillespie, P. A., Fisher, Q. J., Halvorsen, T., Knipe, R. J., 2002. Empirical estimation of fault rock properties: In Norwegian Petroleum Society Special Publications (Vol. 11, pp. 109-125). Elsevier.

Storck, J. C., Brack, P., Wotzlaw, J. F., Ulmer, P., 2019. Timing and evolution of Middle Triassic magmatism in the Southern Alps (northern Italy). Journal of the Geological Society, 176(2), 253-268.

Storti, F., Billi, A., Salvini, F., 2003. Particle size distributions in natural carbonate fault rocks: insights for non-self-similar cataclasis: Earth and Planetary Science Letters, 206(1-2), 173-186.

Storti, F., Balsamo, F., Salvini, F., 2007. Particle shape evolution in natural carbonate granular wear material. Terra Nova, 19(5), 344-352.

Tan, S. C., Zhou, J. X., Li, B., Zhao, J. X., 2017. In situ Pb and bulk Sr isotope analysis of the Yinchanggou Pb-Zn deposit in Sichuan Province (SW China): Constraints on the origin and evolution of hydrothermal fluids. Ore Geology Reviews. 91, 432-443.

Tang, C. A., Liu, H., Lee, P. K. K., Tsui, Y., Tham, L., 2000. Numerical studies of the influence of microstructure on rock failure in uniaxial compression—part I: effect of heterogeneity. International Journal of Rock Mechanics and Mining Sciences, 37(4), 555-569.

Tartaglia, G., Viola, G., van der Lelij, R., Scheiber, T., Ceccato, A., Schönenberger, J., 2020. "Brittle structural facies" analysis: A diagnostic method to unravel and date multiple slip events of long-lived faults: Earth and Planetary Science Letters, v. 545, p. 116420.

Tchalenko, J. S., 1970. Similarities between shear zones of different magnitudes. Geological Society of America Bulletin, 81(6), 1625-1640.

Tepp, G., 2021. Material failure and caldera collapse: insights from the 2018 Kilauea eruption. Earth Planet Sci. Lett. 553, 116621 https://doi.org/10.1016/j.epsl.2020.116621.

Tesei, T., Collettini, C., Viti, C., Barchi, M. R., 2013. Fault architecture and deformation mechanisms in exhumed analogues of seismogenic carbonate-bearing thrusts: Journal of Structural Geology, v. 55, p. 167-181.

Tibaldi, A., Groppelli, G., 2002. Volcano-tectonic activity along structures of the unstable NE flank of Mt. Etna (Italy) and their possible origin. Journal of Volcanology and Geothermal Research, 115(3-4), 277-302.

Tibaldi, A., Groppelli, G., 2002. Volcano-tectonic activity along structures of the unstable NE flank of Mt. Etna (Italy) and their possible origin. J. Volcanol. Geoth. Res. 115 (3–4), 277–302. https://doi.org/10.1016/S0377-0273(01)00305-5.

Tomassi, A., Trippetta, F., de Franco, R., Ruggieri, R., 2023. How petrophysical properties influence the seismic signature of carbonate fault damage zone: Insights from forward-seismic modelling: Journal of Structural Geology, 104802.

Tondi, E., 2007. Nucleation, development and petrophysical properties of faults in carbonate grainstones: evidence from the San Vito Lo Capo peninsula (Sicily, Italy): Journal of Structural Geology, v. 29(4), p. 614-628.

Tondi, E., Antonellini, M., Aydin, A., Marchegiani, L., Cello, G., 2006. The role of deformation bands, stylolites and sheared stylolites in fault development in carbonate grainstones of Majella Mountain, Italy: Journal of structural geology, v. 28(3), p. 376-391.

Torabi, A., Fossen, H., Braathen, A., 2013. Insight into petrophysical properties of deformed sandstone reservoirs: AAPG Bulletin, 97(4), 619-637.

Torabi, A., Alaei, B., Ellingsen, T. S. S., 2018. Faults and fractures in basement rocks, their architecture, petrophysical and mechanical properties: Journal of Structural Geology, v. 117, p.

256-263.

Torabi, A., Ellingsen, T. S. S., Johannessen, M. U., Alaei, B., Rotevatn, A., Chiarella, D., 2020. Fault zone architecture and its scaling laws: where does the damage zone start and stop?: Geological Society, London, Special Publications, 496(1), 99-124.

Trippanera, D., Acocella, V., Ruch, J., Abebe, B., 2015. Fault and graben growth along active magmatic divergent plate boundaries in Iceland and Ethiopia. Tectonics 34(11), 2318–2348. https://doi.org/10.1002/2014JB011850.

Trippanera, D., Ruch, J., Passone, L., Jonsson, S., 2019. Structural mapping of dike-induced faulting in Harrat Lunayyir (Saudi Arabia) by using high resolution drone imagery. Front. Earth Sci. 7, 168. https://doi.org/10.3389/feart.2019.00168.

Troiano, A., Isaia, R., Di Giuseppe, M.G., Tramparulo, F.D.A., Vitale, S., 2019. Deep electrical resistivity tomography for a 3D picture of the most active sector of Campi Flegrei caldera. Sci. Rep. 9 (1), 15124 https://doi.org/10.1038/s41598-019-51568-0.

Tucker, M.E. Wright, V. P., 1990. Carbonate Sedimentology, Blackwell Scientific Publications.

Tuffen, H., Dingwell, D., 2005. Fault textures in volcanic conduits: evidence for seismic trigger mechanisms during silicic eruptions. Bulletin of Volcanology, 67, 370-387.

Turcotte, D. L., Schubert, G., 2002. Geodynamics. Cambridge university press.

UNI EN 14579, 2005. Natural Stone Test Methods-Determination of Sound Speed Propagation, CNR-ICR, Rome.

Vaccaro, C., Atzori, P., Del Moro, A., Oddone, M., Tarversa, G., Villa, I., 1991. Geochronology and Sr isotope geochemistry of late-Hercynian dykes from Sardinia. Schweizerische mineralogische und petrographische Mitteilungen, 71, 221-230.

Valente, E., Ascione, A., Buscher, J. T., Mazzoli, S., Petrosino, P., 2018. Active tectonics in the southern Matese area: insights from geomorphological, morphometrical, stratigraphical, structural and tephrostratigraphical data. In: Rendiconti Online della Società Geologia Italiana (p. 300).

Valente, E., Buscher, J. T., Jourdan, F., Petrosino, P., Reddy, S. M., Tavani, S., Corradetti, E., Ascione, A., 2019. Constraining mountain front tectonic activity in extensional setting from geomorphology and Quaternary stratigraphy: A case study from the Matese ridge, southern

Apennines. Quaternary Science Reviews. 219, 47-67.

Vandeginste, V., Swennen, R., Gleeson, S.A., Ellam, R.M., Osadetz, K. Roure, F., 2005. Zebra dolomitization as a result of focused fluid flow in the Rocky Mountains Fold and Thrust Belt, Canada. Sedimentology. 52, 1067-1095.

Ventura, G., Vilardo, G., 1999. Seismic-based estimate of hydraulic parameters at Vesuvius Volcano. Geophysical research letters, 26(7), 887-890.

Visonà, D., Zanferrari, A., 2000. Some constraints on geochemical features in the Triassic mantle of the easternmost Austroalpine-Southalpine domain: evidence from the Karawanken pluton (Carinthia, Austria). International Journal of Earth Sciences: Geologische Rundschau, 89(1), 40.

Vitale, S., Albanese, S., Di Maio, R., Ambrosino, M., Cicchella, D., De Paola, C., Fabozzi, C., Notaro, P., Pagliara, F., Prinzi, E. P., Ciarcia, S., 2023. Insights on the active Southern Matese Fault system through geological, geochemical, and geophysical investigations of the CO2 gas vent in the Solopaca area (southern Apennines, Italy). Tectonophysics, 846, 229657.

Vitale, S., Ciarcia, S., 2013. Tectono-stratigraphic and kinematic evolution of the southern Apennines/Calabria–Peloritani Terrane system (Italy). Tectonophysics 583, 164–182. https://doi.org/10.1016/j.tecto.2012.11.004.

Vitale, S., Isaia, R., 2014. Fractures and faults in volcanic rocks (Campi Flegrei, southern Italy): insight into volcano-tectonic processes. Int. J. Earth Sci. 103 (3), 801–819. https://doi.org/10.1007/s00531-013-0979-0.

Vitale, S., Ciarcia, S., 2022. The dismembering of the Adria platforms following the Late Cretaceous-Eocene abortive rift: A review of the tectono-stratigraphic record in the southern Apennines: International Geology Review, v. 64(20), p. 2866-2889.

Vitale, S., Prinzi, E. P., Ciarcia, S., Sabbatino, M., Tramparulo, F. D. A., Verazzo, G., 2019. Polyphase out-of-sequence thrusting and occurrence of marble detritus within the wedge-top basin deposits in the Mt. Massico (southern Apennines): Insights into the late Miocene tectonic evolution of the central Mediterranean. International Journal of Earth Sciences, 108, 501-519.

Vitale, S., Isaia, R., Ciarcia, S., Giuseppe, M.G.D., Iannuzzi, E., Prinzi, E.P., Tramparulo, F.D.A., Troiano, A., 2019. Seismically induced soft-sediment deformation phenomena during the volcano-tectonic activity of Campi Flegrei caldera (southern Italy) in the last 15 kyr. Tectonics 38 (6),

1999. https://doi.org/10.1029/2018TC005267,2018.

Vitale, S., Prinzi, E. P., Tramparulo, F. D. A., De Paola, C., Di Maio, R., Piegari, E., Sabbatino, M., Natale, J., Notaro, P., Ciarcia, S., 2020. Late Miocene-early Pliocene out-of-sequence thrusting in the southern Apennines (Italy). Geosciences, 10(8), 301.

Waite, G. P., Smith, R. B., 2002. Seismic evidence for fluid migration accompanying subsidence of the Yellowstone caldera. Journal of Geophysical Research: Solid Earth, 107(B9), ESE-1.

Walker, G.P.L., 1984. Downsag calderas, ring faults, caldera sizes, and incremental caldera growth. J. Geophys. Res. Solid Earth 89 (B10), 8407–8416. https://doi.org/10.1029/JB089iB10p08407

Walker, R. J., Holdsworth, R. E., Armitage, P. J., Faulkner, D. R., 2013. Fault zone permeability structure evolution in basalts. Geology, 41(1), 59-62.

Walsh, J.J., Bailey, W.R., Childs, C., Nicol, A., Bonson, C.G., 2003. Formation of segmented normal faults: a 3-D perspective. J. Struct. Geol. 25 (8), 1251–1262. https://doi.org/10.1016/S0191-8141(02)00161-X.

Walsh, J.J., Watterson, J., 1989. Displacement gradients on fault surfaces. J. Struct. Geol. 11 (3), 307 316. https://doi.org/10.1016/0191-8141(89)90070-9.

Walsh, J.J., Watterson, J., 1991. Geometric and kinematic coherence and scale effects in normal fault systems. Geol. Soc.London.Special Publ 56 (1), 193–203. https://doi.org/10.1144/GSL.SP.1991.056.01.13.

Walter, T.R., Acocella, V., Neri, M., Amelung, F., 2005. Feedback processes between magmatic events and flank movement at Mount Etna (Italy) during the 2002–2003 eruption. J. Geophys. Res. Solid Earth 110 (B10). https://doi.org/10.1029/2005JB003688.

Wang, Z., Wang, T., Wu, S., Hao, Y., 2021. Investigation into the effects of grain size on strength and failure behaviors of granites using a breakable polygonal grain–based model. Bulletin of Engineering Geology and the Environment, 80, 6989-7007.

Warren, J., 2000. Dolomite: occurrence, evolution and economically important associations. Earth-Science Reviews. 52(1-3), 1-81.

Watkins, H., Bond, C. E., Healy, D., Butler, R. W., 2015. Appraisal of fracture sampling methods and a new workflow to characterise heterogeneous fracture networks at outcrop: Journal of

Structural Geology, v. 72, p. 67-82.

Wawersik, W. R., Brace, W. F., 1971. Post-failure behavior of a granite and diabase. Rock mechanics, 3, 61-85.

Wesnousky, S. G., 1986. Earthquakes, Quaternary faults, and seismic hazard in California. Journal of Geophysical Research: Solid Earth, 91(B12), 12587-12631.

Westoby, M.J., Brasington, J., Glasser, N.F., Hambrey, M.J., Reynolds, J.M., 2012. 'Structure-from-Motion'photogrammetry: a low-cost, effective tool for geoscience applications. Geomorphology 179, 300–314. https://doi.org/10.1016/j.geomorph.2012.08.021.

Whalen, J. B., Gariepy, C., 1986. Petrogenesis of the McGerrigle plutonic complex. Gaspe, Quebec: A preliminary report. Geological Survey of Canada, Paper, 265-274.

White, R. S., Drew, J., Martens, H. R., Key, J., Soosalu, H., Jakobsdóttir, S. S., 2011. Dynamics of dyke intrusion in the mid-crust of Iceland. Earth and Planetary Science Letters, 304(3-4), 300-312.

Whittaker, A. C., 2012. How do landscapes record tectonics and climate?. Lithosphere, 4(2), 160-164.

Wibberley, C. A., Gonzalez-Dunia, J., Billon, O., 2017. Faults as barriers or channels to production-related flow: insights from case studies. Petroleum Geoscience, 23(1), 134-147.

Wicks, C., de La Llera, J. C., Lara, L. E., Lowenstern, J., 2011. The role of dyking and fault control in the rapid onset of eruption at Chaitén volcano, Chile. Nature, 478(7369), 374-377.

Willis, B., 1894. The mechanics of Appalachian structure: US Government Printing Office.

Wilson, E. N., Hardie, L. A., Phillips, O. M., 1990. Dolomitization front geometry, fluid flow patterns, and the origin of massive dolomite: the Triassic Latemar buildup, northern Italy. American Journal of Science, 290(7), 741-796.

Wong, R. H., Chau, K. T., Wang, P., 1996. Microcracking and grain size effect in Yuen Long marbles. In International journal of rock mechanics and mining sciences & geomechanics abstracts (Vol. 33, No. 5, pp. 479-485).

Wong, T. F., Szeto, H., Zhang, J., 1992. Effect of loading path and porosity on the failure mode of porous rocks: Applied Mechanics Reviews, v. 45(8), p. 281-293.

Wong, T. F., David, C., Zhu, W., 1997. The transition from brittle faulting to cataclastic flow in porous sandstones: Mechanical deformation: Journal of Geophysical Research: Solid Earth, v. 102(B2), p. 3009-3025.

Wong, T. F., Wong, R. H., Chau, K. T., Tang, C. A., 2006. Microcrack statistics, Weibull distribution and micromechanical modeling of compressive failure in rock. Mechanics of Materials, 38(7), 664-681.

Woodcock, N. H., Mort, K., 2008. Classification of fault breccias and related fault rocks. Geological Magazine, 145(3), 435-440.

Wu, J., Wang, Q., Cheng, X., Cheng, F., Yu, X., Zhang, C., Shen, X. Guo, Z., 2023. Formation of multi-stage and clustered fractures at 3.6–4.9 km in the Shizigou structure, SW Qaidam basin: Journal of Structural Geology, v. 169, p. 104845.

Yang, T., Azmy, K., He, Z., Li, S., Liu, E., Wu, S., Wang, J., Li, T., Gao, J., 2022. Fault-controlled hydrothermal dolomitization of Middle Permian in southeastern Sichuan Basin, SW China, and its temporal relationship with the Emeishan Large Igneous Province: New insights from multi-geochemical proxies and carbonate U–Pb dating. Sedimentary Geology, 439, 106215.

Yu, Q., Zhu, W., Ranjith, P. G., Shao, S., 2018. Numerical simulation and interpretation of the grain size effect on rock strength. Geomechanics and Geophysics for Geo-Energy and Geo-Resources, 4, 157-173.

Zanetti, A., Mazzucchelli, M., Sinigoi, S., Giovanardi, T., Peressini, G., Fanning, M., 2013. SHRIMP U–Pb zircon Triassic intrusion age of the Finero mafic complex (Ivrea–Verbano Zone, Western Alps) and its geodynamic implications. Journal of Petrology, 54(11), 2235-2265.

Zavattieri, P. D., Espinosa, H. D., 2001. Grain level analysis of crack initiation and propagation in brittle materials. Acta Materialia, 49(20), 4291-4311.

Zempolich, W. G., Hardie, L. A., 1997. Geometry of dolomite bodies within deep-water resedimented oolite of the Middle Jurassic Vajont Limestone, Venetian Alps, Italy: Analogs for hydrocarbon reservoirs created through fault-related burial dolomitization. In: Kupecz, J. A., Gluyas, J., Bloch, S., 1997. (Eds), Reservoir Quality Prediction in Sandstones and Carbonates. AAPG Memoir. 69, 127-162.

Zhang, J., Wong, T. F., Davis, D. M., 1990. Micromechanics of pressure-induced grain crushing in porous rocks: Journal of Geophysical Research: Solid Earth, v. 95(B1), p. 341-352.

Zhang, L., 2010. Estimating the strength of jointed rock masses: Rock Mechanics and Rock Engineering, v. 43, p. 391-402.

Zhang, W., Hu, Z., 2020. Estimation of Isotopic Reference Values for Pure Materials and Geological Reference Materials. Atomic Spectroscopy. 41(3), 93-102. doi: 10.46770/AS.2020.03.001

Zhao J, Zhou Y, Hefny A, Cai J, Chen S, Li H, et al. 1999. Rock dynamics research related to cavern development for ammunition storage. Tunn Undergr Space Technol, 14, 513–26.

Zhao, X., Elsworth, D., He, Y., Hu, W., Wang, T., 2021. A grain texture model to investigate effects of grain shape and orientation on macro-mechanical behavior of crystalline rock. International Journal of Rock Mechanics and Mining Sciences, 148, 104971.

Zhao, Z., Dong, C., Ma, P., Lin, C., Li, G., Du, X., Luan, G., He, Y., Liu, W., 2022. Origin of Dolomite in Lacustrine Organic-Rich Shale: A Case Study in the Shahejie Formation of the Dongying Sag, Bohai Bay Basin. Frontiers in Earth Science. 10, 909-107. doi: 10.3389/feart.2022.909107.